Cost-effective membrane technologies for carbon dioxide capture – membrane processes for amine contaminant removal: Final Report

ANLEC Project No. 3-0510-0045

Josephine Lim, Alita Aguiar, Ludovic Dumée, Geoff Stevens, Colin Scholes, Dianne Wiley, Sandra Kentish

March 2014 | CO2CRC Report No: RPT14-4873

REPORT

STUDIES IN CCS

THE UNIVERSITY OF MELBOURNE

CO2CRC PARTICIPANTS

Core Research Participants

CSIRO
Curtin University
Geoscience Australia
GNS Science
Monash University
Simon Fraser University
University of Adelaide
University of Melbourne
University of New South Wales
University of Western Australia

Industry & Government Participants

ANLEC R&D
BG Group
BHP Billiton
BP Developments Australia
Brown Coal Innovation Australia
Chevron
State Government Victoria – Dept. of State Development Business & Innovation
INPEX
KIGAM
NSW Government Dept. Trade & Investment
Rio Tinto
SASOL
Shell
Total
Western Australia Dept. of Mines and Petroleum
Glencore

Supporting Participants

CanSyd Australia
Charles Darwin University
Government of South Australia
Lawrence Berkeley National Laboratory
Process Group
The Global CCS Institute
University of Queensland

An Australian Government Initiative

CRC AUSTRALIA

Cost-effective membrane technologies for carbon dioxide capture – membrane processes for amine contaminant removal: Final Report

ANLEC Project No. 3-0510-0045

Josephine Lim, Alita Aguiar, Ludovic Dumée, Geoff Stevens, Colin Scholes, Dianne Wiley, Sandra Kentish

March 2014
CO2CRC Report RPT14-4873

CO2CRC

THE UNIVERSITY OF MELBOURNE

Acknowledgements

The authors acknowledge the financial support provided by the Australian Government through its Cooperative Research Centre program for this CO2CRC research project. The authors also acknowledge financial assistance provided through Australian National Low Emissions Coal Research Development (ANLEC R&D). ANLEC R&D is supported by Australian Coal Association Low Emission Technology Limited and the Australian Government through the Clean Energy Initiative.

Cooperative Research Centre for Greenhouse Gas Technologies (CO2CRC)

GPO Box 463
Ground Floor NFF House, 14-16 Brisbane Avenue, Barton ACT 2600
CANBERRA ACT 2601
Phone: +61 2 6120 1600
Fax: +61 2 6273 7181
Email: info@co2crc.com.au
Web: www.co2crc.com.au

Reference**: Lim, J., Aguiar, A., Dumee, L, Stevens, G, Scholes, C, Wiley, D**, **and Kentish, S.** 2014. *Cost-Effective Membrane Technologies for Carbon Dioxide Capture - Membrane Processes for Amine Contaminant Removal: Final Report. ANLEC report*. Cooperative Research Centre for Greenhouse Gas Technologies, Canberra, Australia, CO2CRC Publication Number RPT14-4873. 66 pp.

Executive summary

Monoethanolamine (MEA) is commonly used in natural gas sweetening to selectively absorb CO_2 from a mixed gas stream. It has high CO_2 loading capacity and the reactions are fast compared to other amine based solvents. When applied to post-combustion capture, a major drawback from this operation is the formation of heat stable salts (sulfates, oxalates, acetates, nitrates and other species), which result from the parasitic reactions between MEA and other impurities (especially SO_2, and NO_2) in the feed gas stream. Since the formation of heat stable salts (HSS) can lead to corrosion and high viscosities, a fraction of the degraded solvent must be continuously purged from the system and replaced with fresh solvent.

In this project, the potential use of nanofiltration (NF) and electrodialysis (ED) as an in-situ treatment of degraded MEA solution is investigated. The aim is to separate the heat stable salts from the system hence minimising the cost of CO_2 capture by reducing the amount of fresh solvent make-up required, the extent of corrosion and the cost of waste disposal.

The results with pure MEA solutions show that nanofiltration can be used to remove up to 90 % of sulphates and oxalates from a 30 wt% MEA solution using a KOCH SeIRO MPF-34 membrane. Further testing using a smaller pore size membrane may achieve a better separation of these smaller heat stable salts.

A high salt removal can also be achieved by electrodialysis, when operated in a batch mode. In a continuous mode, the extent of the HSS removal can be related to the applied current density, the salt being removed, the flowrate through the unit, the membrane type and the effective membrane area. In order to reduce the operating costs associated with power consumption and membrane area, it is important to use a membrane that exhibits a low electrical resistance and a solution that contains relatively high levels of heat stable salts. Neosepta membranes were found to be the most effective of the three supplier types trialled.

In the final stage of the project, MEA that has been used in pilot scale carbon capture operations has been obtained through a collaboration with CSIRO. Solutions that had been aged for 50+ and 1800+ hours were the focus of this work. The 50+ solution was at a high CO_2 loading and this was initially reduced through simple boiling, as our early work had shown that neither NF or ED is effective at high loadings. The solutions were first neutralised with sodium hydroxide to free amine-bound salts. This resulted in the formation of precipitates, which were removed using a microfiltration membrane.

Nanofiltration of the aged solutions proved ineffective. The MEA rejection, which had been low in initial experiments increased; while the salt rejection, high in initial experiments declined. The flux through the membrane also declined significantly. These results reflect the non-zero CO_2 loading of the solution. Conversely, electrodialysis remained an effective approach to remove heat stable salts. Over 90 % of these salts could be removed from the solution, with time constraints only preventing further removal. The heat stable salts were found to be predominantly sulfates and nitrates.

Table of Contents

List of tables

List of figures

Publications

L. Dumee, G. Stevens, S. Kentish, Purification of aqueous amine solvents used in post combustion CO_2 capture: A review, International Journal of Greenhouse Gas Control, 10 (2012) 443–455.

S. E. Kentish, E. Kloester, G. W. Stevens, C. A. Scholes, L. Dumée, Electrodialysis in aqueous-organic mixtures, submitted to Separation and Purification Reviews

Introduction

In spite of the emergence of greener energy resources, fossil fuel combustion remains a major source for energy production in the 21st century due to the well established knowledge of the operation and the number of existing plants. With the amount of CO_2 generated, the operation is also related to increasing global warming and the greenhouse effect. In the past few decades, a number of approaches have been considered to mitigate these greenhouse gas emissions by implementing post-combustion CO_2 capture at fossil fuel power plants.

Among all the post-combustion capture techniques under consideration [1, 2], the most feasible and widely accepted approach is to use an amine such as monoethanolamine (MEA) as a solvent to selectively absorb CO_2 from the flue gas [3-5]. MEA is capable of providing high levels of CO_2 purity and recovery with relatively fast kinetics. This performance is strongly related to the bonding efficiency between MEA and CO_2 to form carbamate anions and protonated amines (Scheme 1).

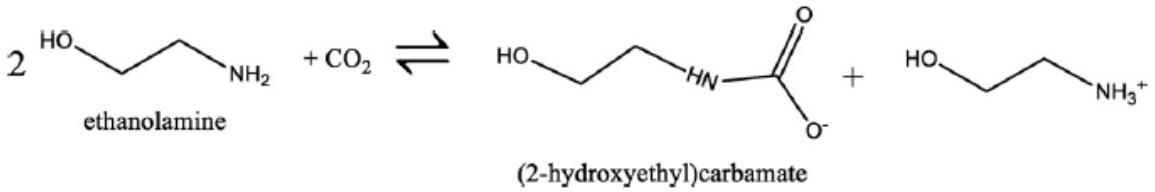

Scheme 1 - Reaction of two MEA molecules with CO_2 to form the carbamate anion and a protonated amine

However, parasitic reactions can occur during post-combustion capture due to the presence of impurities in the flue gas. The reaction between MEA and these impurities may result in the formation of heat stable salts (HSS), which are difficult to regenerate and cause an increase in the viscosity of the solvent and corrosion to the operating units [6-8]. These heat stable salts can include organic acids such as acetic and oxalic acid, as well as sulfates, sulfites, nitrates, nitrates which form by irreversible reactions (Scheme 2) with free amine [9]. Interaction with corrosion by-products can lead to a range of metal cations with these salts. It was confirmed in previous studies that the presence of only 500 ppm (mg/litre) of amine degradation products may increase corrosion rates by fifty-fold [6, 10].

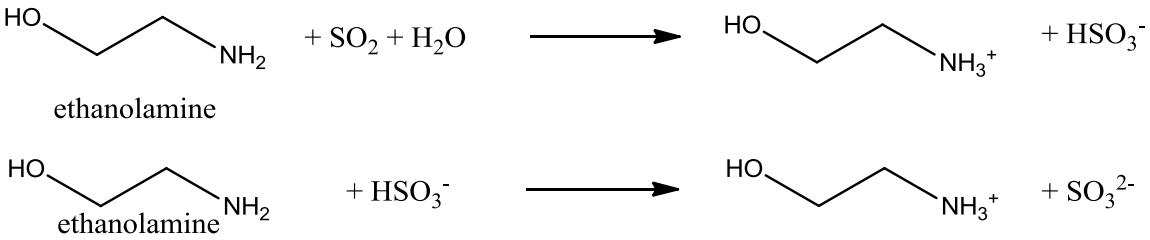

Scheme 2 – Reaction of MEA with sulfur dioxide to form bisulfite and sulfite heat stable salts

Additionally, neutral species and oligomers can also be formed through thermal degradation and polymerisation of amine species [11, 12]. These contaminants reduce the amount of active amine available for CO_2 capture. Solution viscosity also increases as the concentration of contaminants increases, which in turn increases the energy demand and reduces the carbon dioxide recovery due to reduced kinetics.

To overcome these issues, a fraction of degraded MEA needs to be purged and replaced with fresh MEA thus increasing the maintenance cost for all unit operations and the operating cost for solvent replacement [8]. For example, the financial loss due to ethanolamine degradation, evaporation at the top of the stripper column and HSS concentration build-up may reach up to US$ 8 M / year for a 1 Mm^3 / year CO_2 capture plant [13, 14]. Alternatively, the trapped amine species can be released by neutralising the acidic contaminants using a carbonate salt, sodium hydroxide or potassium hydroxide [15]. However, neutralisation alone can lead to precipitation of less soluble salts, causing fouling or foaming in the downstream processes [8]. Thermal reclamation can also be used, whereby MEA is distilled from the unwanted salts and oligomers, leaving a waste sludge. Nonetheless, this approach leads to significant MEA losses and a large volume of waste sludge requiring disposal [16].

A membrane-based separation technology, electrodialysis, has also been considered as a method to purify contaminated MEA solvent [17, 18]. A patent for recovering alkanolamines was issued to the Dow Chemical Company in the 1980s [19] and an on-line purification process for MEA using electrodialysis (also known as UCARSEP® process) was developed by Union Carbide in the late 80s to early 90s. The method can provide high HSS removal and high amine recovery [18, 20]. However, the solution must still first be neutralized, and the application is limited to the removal of charged contaminants only. Additional treatments are required to remove the neutral species and oligomers, which are also generated during the MEA scrubbing process. Ion exchange is another approach that can be used in a comparable manner.

Approaches such as thermal reclamation and electrodialysis are most effective when the concentration of contaminants is relatively high (> 1 wt% or 10,000 ppm [18, 20]). For this reason, reclamation is often carried out in a batch mode, with a reclamation unit brought on site on a temporary basis to improve solvent quality. However, it would be much more practical if a continuous online reclamation process were to be implemented for flue gas capture, due to the large volumes of solution to be treated.

More details of the approaches to amine reclamation are provided in our published paper [9].

In this project, an in-situ purification of MEA using a sequence of nanofiltration and electrodialysis is investigated. This approach is expected to be more efficient compared to existing technologies that often rely on the single use of ion exchange, vacuum distillation or electrodialysis. The novelty is the pre-treatment of the contaminated MEA slip-stream using nanofiltration prior to electrodialysis. A schematic of the proposed flowsheet is provided in Figure 1.

Nanofiltration (NF) is considered as a mechanism for concentrating the heat stable salts within an amine solution, following neutralisation. If effective, such an approach would allow the carbon capture process to operate with low HSS concentrations (e.g. 500 - 1000 ppm) while continuously delivering a lower volume and more concentrated solution to a downstream thermal reclamation or electrodialysis process.

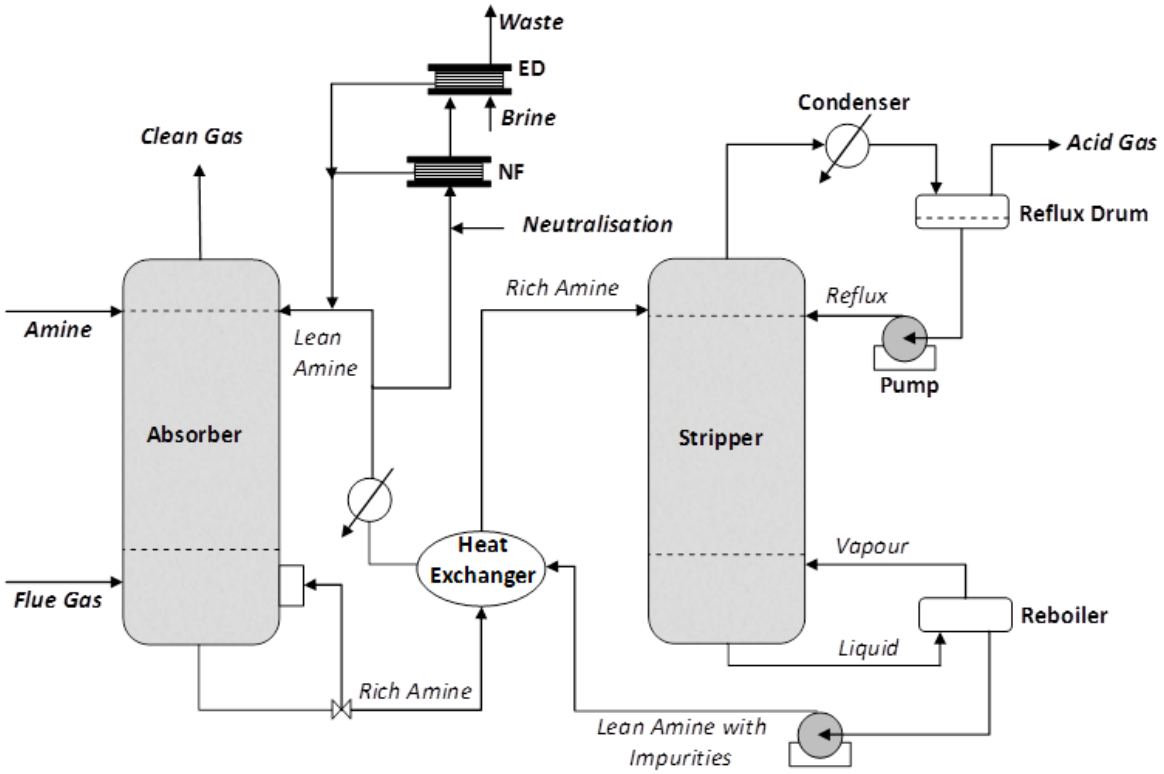

Figure 1 – A process schematic of how nanofiltration could be incorporated into a post combustion capture process to maintain total MEA impurity levels at around 1000 ppm (1 g/litre). A slipstream of MEA solvent is reclaimed through consecutive operations of neutralization, nanofiltration and electrodialysis.

The approach taken involves testing a series of model solutions with different HSS content on a NF and ED lab-scale rig using a number of commercially available membranes. The investigation focuses on 30 wt% MEA / water solutions, which represents the typical composition of industrial solvent. Experiments using industrial amine solvents of around 25 wt% MEA (from the CSIRO post-combustion CO_2 capture plant at Loy Yang power station) were also conducted to evaluate the processes under more severe conditions.

The aim of the study is to find a process that concentrates heat stable salts and thus reduces the viscosity and corrosivity of the circulating MEA solvent. In turn, this should reduce the maintenance costs and the energy input of the CO_2 capture process.

Nanofiltration (NF)

Nanofiltration is a membrane filtration process, which utilises a pressure drop across the membrane (trans-membrane pressure) as a driving force to separate ions or uncharged molecules based on their size difference and their charge.

Due to the simultaneous improvement of the membrane chemistry and the substantial decrease in the membrane production costs, NF is progressively emerging as an integrated purification solution for many industrial applications [21-24]. With a typical molecular cut-off membrane between 200 and 1000 Daltons, NF has the potential to prevent most macro-molecules from permeating through the membrane.

The application of NF as an efficient and low cost technique in water softening [25] and acid removal [26-28] has been demonstrated. Additionally, NF has been increasingly used in the past decade for the treatment and purification of organic co-solvents [29].

Previous studies show that the rejection of MEA in a 5 wt% MEA solution can be as high as 70 % at low pH operations [30]. However, in the present case, the aim is to run the NF operation at high pH. By maintaining the pH above 11, the MEA is predominantly uncharged and should permeate through the membrane. Conversely, charged contaminants and higher molecular weight uncharged species should be retained. Ultimately, this should lead to a concentrated retained waste solution that can be further processed using other approaches. Simultaneously, a purified MEA solution should be collected as permeate and returned directly to the main CO_2 capture process.

Experimental details for NF

Materials for NF

Samples were prepared by mixing laboratory grade oxalic acid dihydrate ($C_2H_2O_4.2H_2O$, 99.5 %, Merck), acetic acid ($C_2H_4O_2$, 99.7 %, Chem-Supply), sulfuric acid (H_2SO_4, 95 – 97 %, Scharlau), or nitric acid (HNO_3, 70 wt%, Ajax FineChem) with Reverse Osmosis (RO) water and either pure monoethanolamine (MEA, 99.5 %, Chem-Supply) or sodium hydroxide (5 M), using a magnetic stirrer for five minutes. The concentration of the acids and MEA was kept constant at 500 ppm (mg/litre) and 30 wt% respectively; in some experiments NaOH was used in place of MEA to adjust the pH to the range 12.4 ± 0.1.

In most experiments, the CO_2 loading was kept at a minimum by preparing the samples in closed containers. In this case, the CO_2 loading of the samples at the end of the tests was always less than 0.02 mol CO_2 / mol MEA. Additionally, CO_2 loaded samples were prepared by bubbling industrial grade CO_2 (99.9 %, BOC) at 15 psi through 30 wt% MEA solutions. The bubbling time was varied to obtain samples with different CO_2 loadings.

Flat sheet membranes SelRO® MPF-34 and SelRO® MPF-36 (proprietary composite) were purchased from Koch Membrane Systems, United Kingdom. As an acid/base stable NF membrane, both membranes have a typical operating pressure of 200 - 510 psi (14 - 35 bar). The pore size, pH range and typical flux for each membrane are listed in Table 1.

Table 1 - Technical data sheet for SeIRO® MPF-34 and MPF-36 membranes (MWCO = Molecular Weight Cut Off)

Membranes	MWCO (Dalton)	pH range (at 25 °C)	Typical flux* (kg/m^2.s)
SeIRO® MPF-34	200	0-14	0.017 at 3000 kPa
SeIRO® MPF-36	1000	1-13	0.056 at 3000 kPa

*Test conditions: 5 % NaCl at 30 °C

In order to remove any chemical residue on the surface, new membranes were soaked overnight and rinsed with RO-water. The membranes were then compressed at 3000 kPa for at least 6 h prior to use. The water permeance of any used membrane was also checked prior to each run to ensure that the membranes were still in good condition.

All nanofiltration tests were conducted using a Sepa CF Membrane Element Cell purchased from Sterlitech Corporation, USA. The cross-flow filtration unit has a membrane active surface area of 140 cm^2 and the thickness of the feed and permeate spacers used is 1.2 and 0.35 mm respectively.

Experimental procedures for NF

The feed solution (2 L) was re-circulated through the NF cell at a flow rate of 1.5 L/min using a centrifugal pump (Figure 2). With a back pressure controller located at the concentrate outlet of the NF cell, the trans-membrane pressure across the membrane was adjusted to 1000, 2000 or 3000 kPa. The permeate flowrate was continuously recorded by a mass balance (A&D Weighing, GF-400 series) and then returned to the feed tank at regular intervals. A small amount of permeate was taken at each trans-membrane pressure for further analysis.

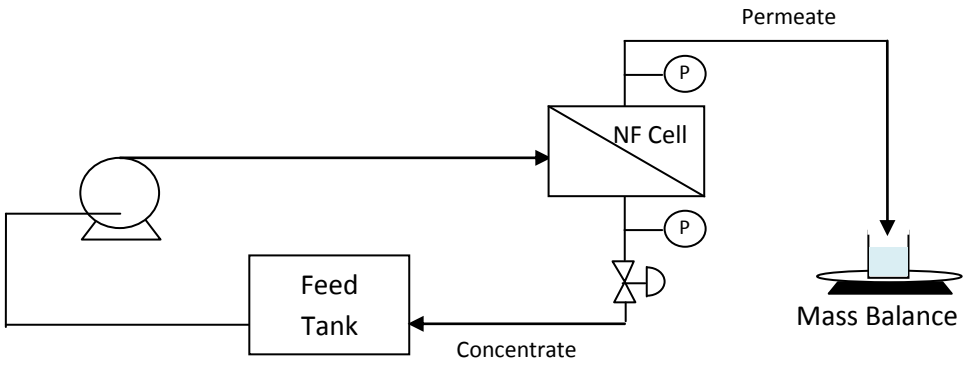

Figure 2 – Schematic diagram of the NF experiment

The rejection of HSS anions can be calculated using the following equation:

$$\mathscr{R} = (1 - C_p / C_f) \times 100\ \%$$ (Equation 1)

where, $\mathscr{R}$, C_p and C_f are the rejection, permeate concentration and feed concentration respectively.

Analytical methods for NF

In experiments with water as the base solution, the concentration of oxalate, acetate, sulfate and nitrate in the permeate was quantified by measuring the change in the conductivity of the solutions using a TPS WP-81 pH, temperature and conductivity meter purchased from Thermo Fisher Scientific.

For experiments using MEA as the base solution, the concentration of the anions was quantified using ion chromatography (Dionex ICS-1000, AS14 column). During the measurements, different mixtures of carbonate and bicarbonate were used as the eluent: 0.8 mM carbonate and 0.1 mM bicarbonate for oxalate and sulfate analysis; 2.0 mM carbonate and 2.0 mM bicarbonate for nitrate and acetate analysis. This was required to shift the retention time of the relevant anions to exclude the presence of any overlapping peaks with MEA that may result in inaccurate quantitative analysis.

The concentration of MEA was determined by titrating the samples with 0.1 M HCl and 0.1 M NaOH to quantify the amount of free and bound amine respectively [30]. The sum of free and bound amine was taken as the concentration of MEA in the solution.

CO_2 loading was determined by titrating the CO_2 loaded MEA solutions with 2 M HCl solution using a Chittick CO_2 analyser [31]. The osmotic pressure of the solution was determined using an Osmomat O30 osmometer.

The extent of membrane swelling was evaluated by immersion in solutions of varying MEA concentration. The swelling degree was calculated using the following equation:

$$swelling\ degree = [(m_{wet} - m_{dry}) / m_{dry}] \times 100\ \% \qquad \text{(Equation 2)}$$

where, m_{wet} and m_{dry} are the wet mass and dry mass of the membrane respectively. Dry mass is the mass of the membrane prior to soaking. Wet mass is the mass of the membrane after immersion. The wet mass value was measured after sandwiching the soaked membrane with Kimwipes. This was done to remove the excess solution on the membrane surface.

Changes to the membrane chemistry were evaluated by attenuated total reflection Fourier transform infrared spectroscopy (ATR-FTIR) analysis. The spectra were obtained using a PerkinElmer Frontier IR Dual-Range spectrometer equipped with an universal ATR accessory (Diamond/ZnSe crystal) and a PerkinElmer Spectrum software version 10.03.08.0135. Each spectrum was collected from an average of 32 scans with the wave number ranging from 500 to 4000 cm^{-1} at 32 cm^{-1} resolution. A background spectrum was collected at the beginning of each measurement for the purpose of CO_2 and water vapour corrections.

Results and discussion for NF

Solution characterization

The experimentally determined osmotic pressure for a range of MEA solutions is presented in Figure 2. At low concentrations, the data is consistent with the Van't Hoff relationship i.e.:

$$\pi = cRT \qquad \text{(Equation 3)}$$

Where π represents the osmotic pressure, c is the concentration of all species, R is the universal gas constant and T is the temperature in Kelvin. At higher concentrations, the data diverges a little from this relationship. As the Osmometer could not be used beyond 10 wt% MEA, it was not possible to determine the osmotic pressure at 30 wt%, but it is likely to be greater than that predicted from the Van't Hoff relationship of 12,000 kPa. Extrapolation of the experimental data in Figure 2 suggests a value of just under 18,000 kPa.

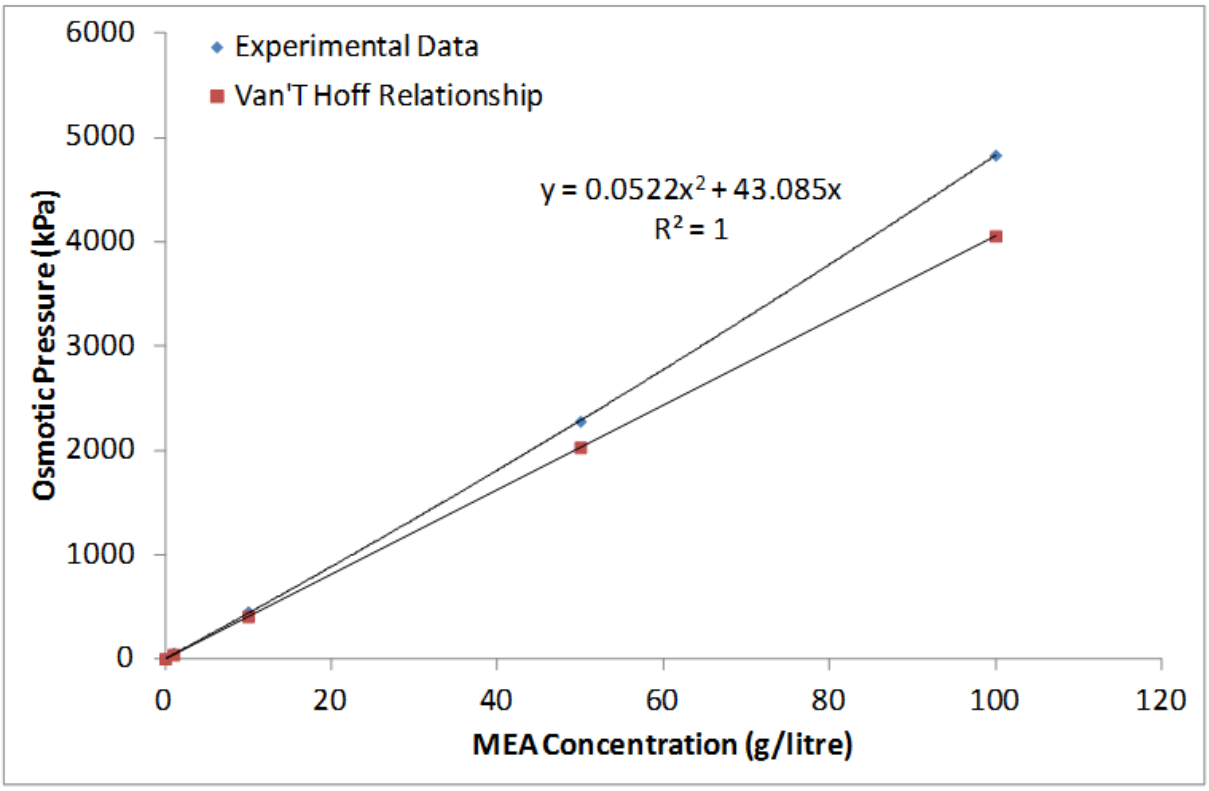

Figure 3 - The osmotic pressure associated with aqueous solutions of monoethanolamine. The experimental results are compared to the well known Van't Hoff relationship.

Nanofiltration results for unloaded MEA

As shown in Table 2, the rejection of MEA by either MPF-34 or MPF-36 membranes is small. This indicates that both membranes can potentially be used to separate heat stable salts from the amine solution. Since the smaller pore size membrane should give a higher rejection of HSS, the following experiments were focused on the MPF-34 membrane.

Table 2 - The rejection of amine species in 30 wt% MEA solution at different pressures using SelRO® MPF-34 and MPF-36 membranes

Pressure (kPa)	Rejection (%)	
	MPF-34	MPF-36
1000	3.1	1.3
2000	4.2	0.6
3000	6.8	0.9

For the MPF-34 membrane, the permeance of 500 ppm solutions of HSS in RO-Water was 1.06 ± 0.3 x 10^{-5} kg/m^2.s.kPa across a full pH range from 2.0 to 12.5. There was no apparent trend in this flux with pH, although there was considerable variability between membrane samples. The average value was significantly higher than the manufacturer's specification of 0.6 x 10^{-5} kg/m^2.s.kPa (Table 1). This reflects the lower salt concentrations (500 mg/litre) for the experiments versus 5 % or 50 g/litre NaCl for the manufacturer's data. With a lower salt concentration, the osmotic pressure is smaller hence the flux is higher. Similarly, the average permeance of 5.9 x 10^{-5} kg/m^2.s.kPa for MPF-36 was higher than the manufacturer specification of 1.9 x 10^{-5} kg/m^2.s.kPa.

In 30 wt% MEA solutions, this permeance fell, reflecting the higher viscosity of these solutions [32]. There was again considerable batch to batch variability, with the average permeance of 1.8 ± 1.0 x 10^{-6} kg/m2.s.kPa across three membrane batches for the MPF-34 membrane. The permeance of 30 wt% MEA through the MPF-36 membrane was 1.5 ± 0.2 x 10^{-5} kg/m^2.s.kPa.

In all experiments, there was a significant osmotic pressure difference that led to a non-zero intercept on the x-axis of a flux versus pressure curve. For the 30 wt% MEA solutions through the MPF-34 membrane, the osmotic pressure difference determined from this intercept was between 200 - 600 kPa, indicating that there is indeed a small rejection of MEA. Given the osmotic pressure of the feed MEA solution is around 18,000 kPa, however, the rejection is small, and equates to a difference in composition between the permeate and feed of around 10 g/litre. That is, the feed solution might increase to 30.5 wt% and the permeate might be 29.5 wt% MEA after permeation. This corresponds to a rejection of around 3% which is consistent with the data presented in Table 2. The calculated osmotic pressure difference for the MPF-36 membrane was 130 kPa, reflecting lower rejection of MEA through this more porous membrane. This is also consistent with the data in Table 2.

The selectivity of the MPF-34 membrane in separating HSS anions from the amine solutions was analysed by measuring the amount of HSS anions present in the permeate using ion chromatography (IC). The results are quantified in terms of rejection and the values are plotted as a function of trans-membrane pressure in Figure 4 and Figure 5.

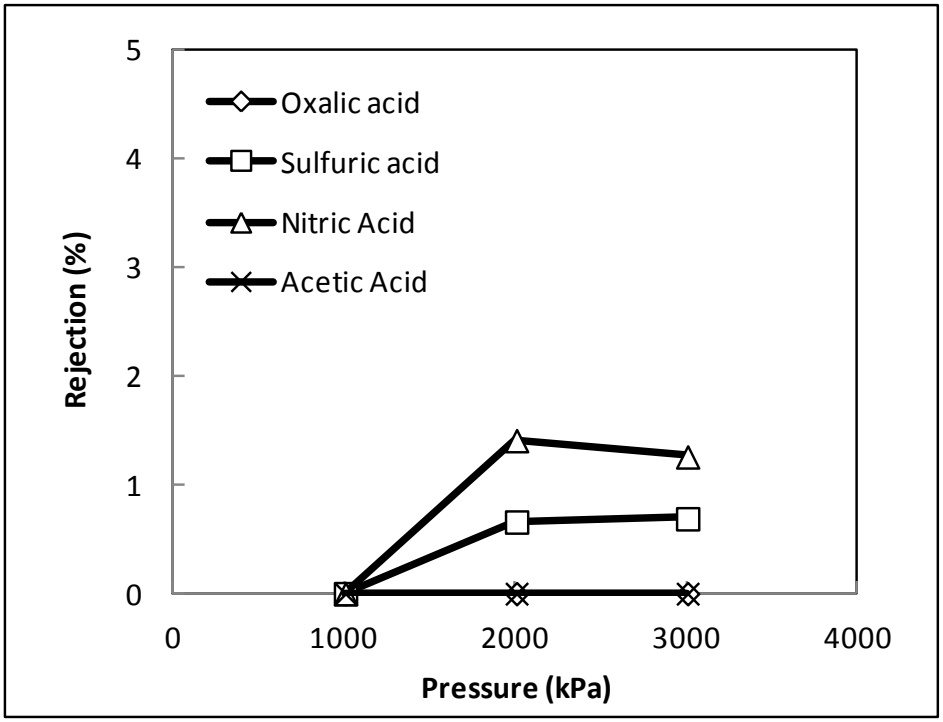

Figure 4 - The rejection of 500 ppm (mg/litre) of a range of acids as a function of trans-membrane pressure, using an MPF-34 membrane in water.

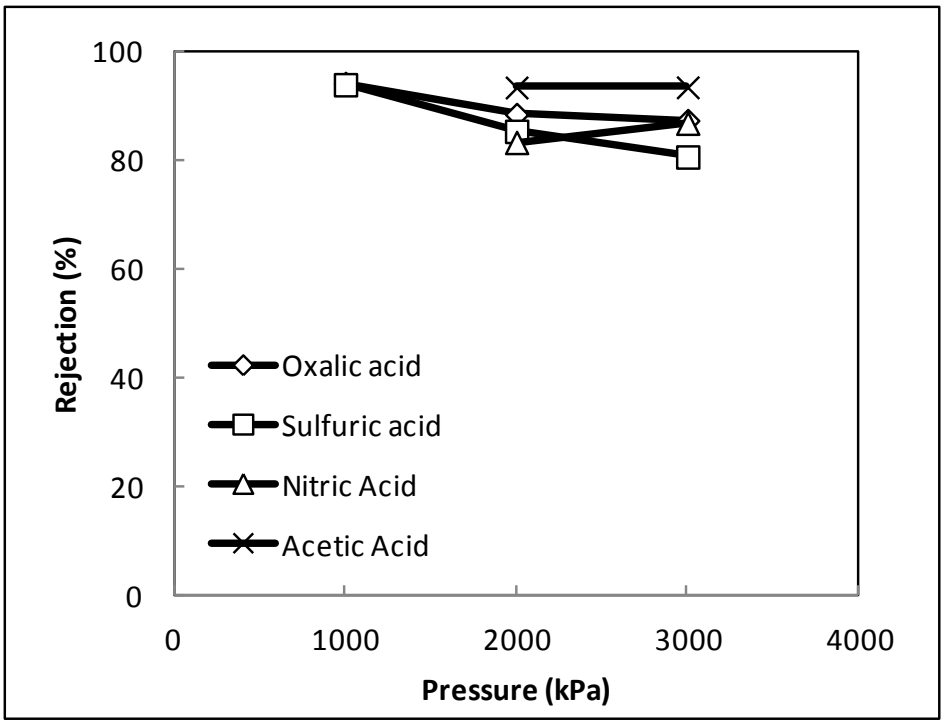

Figure 5 - The rejection of 500 ppm (mg/litre) of a range of acids as a function of trans-membrane pressure, using an MPF-34 membrane in 30 wt% MEA.

The extent of rejection through a NF membrane depends upon the pore size of the membrane relative to the size of the molecular species [33] and the charge differences between the two. In the present case, if the rejection is simply based on the molecular size of the anions, all rejection values should be close to zero since the nominal molecular weight cut off of the membrane is 200 g/mol and the molecular weight of the four anions ranges from 59 g/mol (acetate) to 96 g/mol (sulfate) respectively. Given that the rejection is more than 80% in the 30 wt% MEA system, the rejection of the HSS anions is most likely related to surface charge repulsion, which has been reported to play an important role in membrane separation processes [34-37]. Additionally, the rejection is observed to be essentially independent of the characteristic of the anions due to the similarity in the molecular weight between the species.

The effect of surface charge repulsion on the HSS rejection can be explained by the changes in solution pH. Upon addition of the various acids to water, the pH of the solution was measured to range between 2.05 (sulfuric acid) to 3.8 (acetic acid) depending upon the HSS species present. Under these conditions, the membrane is slightly positively charged and so the anions are readily transmitted through the membrane. As the pH is further increased, the membrane surface becomes increasingly negatively charged [38]. Hence, above neutral pH values, the negatively charged anions are repelled from the membrane (Table 3). This result is in agreement with the prior literature which shows a higher rejection of small organic acids such as formic, oxalic and glycolic, at high pH conditions [39-41].

Table 3 – Rejection of anions from aqueous solution as a function of pH (500 ppm salt concentration, trans-membrane pressure = 2000 kPa, 30°C)

	pH = 2	pH = 10	pH = 12.3
Sulfate	0	87%	96.5%
Nitrate	1.4%	71%	86%

Nanofiltration results for loaded MEA

In practice, the lean loading of the MEA solvent will range between 0.1 – 0.25 mol CO_2 / mol MEA depending on a number of factors such as the operating temperature, the flow rate of the solvent and the characteristic of the absorbing and stripping columns. With the lean loading solvent acting as the feed stream for the NF unit, it is crucial to explore the effect of CO_2 loading on the rejection and permeate flux of HSS-contaminated amine solutions.

As shown in Figure 6 and Figure 7, an increase in CO_2 loading results in a reduction of the permeate flux and an increase in the MEA rejection. This is due to the formation of carbamates and protonated amines when MEA reacts with CO_2 (Scheme 1). These larger charged species are rejected by the membrane. Further, as the CO_2 loading increases up to 0.5 mol CO_2 / mol MEA, the pH of the solution reduces from 11.8 to 7.8, also causing a decline in rejection due to decreasing membrane charge (see Table 3). The greater rejection leads to a significant increase in osmotic pressure, which reduces the permeate flux by an order of magnitude. The loaded

solvent is also more viscous than an unloaded solution, which also contributes to the reduced flux [32, 42].

These findings indicate that for NF to be useful for MEA reclamation, the CO_2 loading would need to be less than 0.2 mol CO_2 / mol MEA. Similarly, the contaminated MEA would need to be 'neutralised' by addition of a strong base such as NaOH, to fully deprotonate the amine and so allow it to permeate the membrane. MEA solutions are traditionally neutralized prior to commercial thermal, ion exchange and electrodialysis based reclamation processes for similar reasons [9].

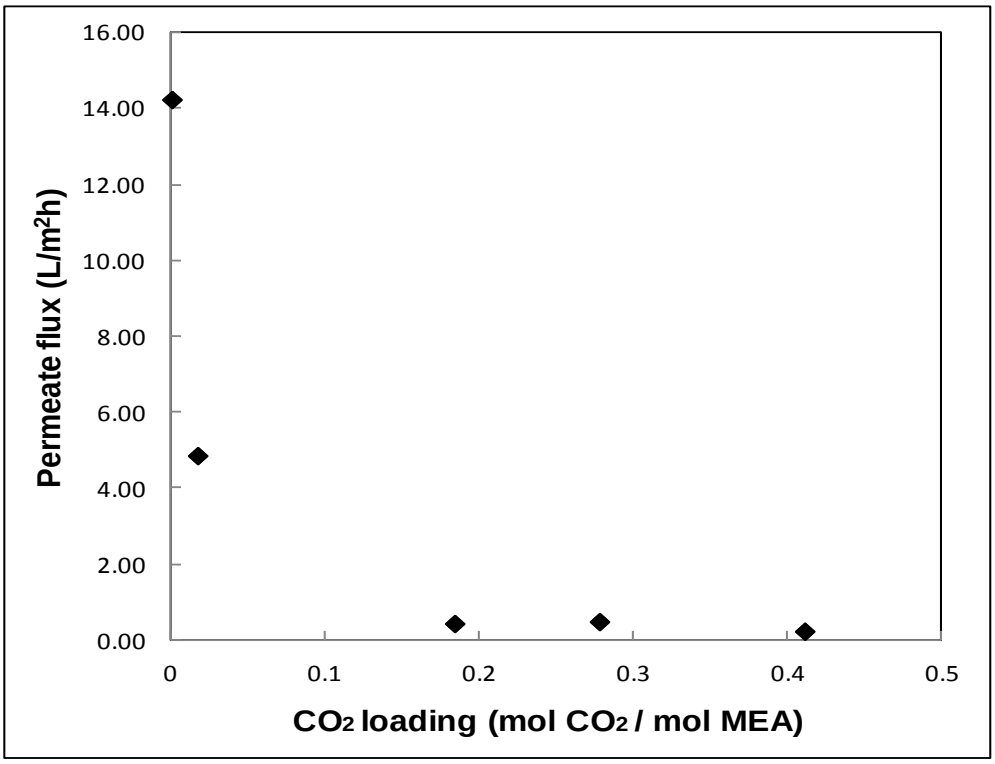

Figure 6 - The permeate flux for a 30 wt% MEA solution through an MPF-34 membrane as a function of the carbon dioxide loading (trans-membrane pressure = 2000 kPa).

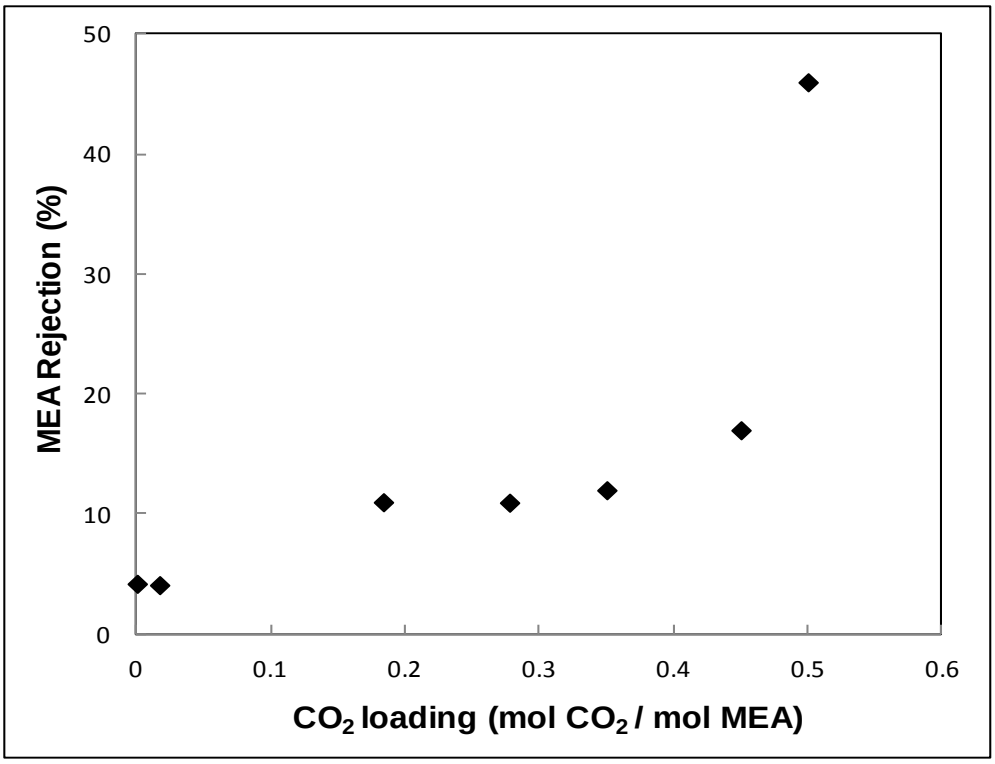

Figure 7 - The MEA rejection for a 30 wt% MEA solution through an MPF-34 membrane as a function of the carbon dioxide loading (trans-membrane pressure = 2000 kPa).

NF membrane stability

The integrity of MPF-34 and MPF-36 membranes for MEA based operation was evaluated by investigating the membrane swelling and the change in membrane composition over time. The extent of membrane swelling was evaluated by immersion in solutions of varying MEA concentration. As shown in Figure 8, even though the membranes swell substantially in water, the extent of swelling does not vary significantly as the concentration of MEA increases. The change in membrane thickness is also observed to be insignificant at any concentration (data not shown).

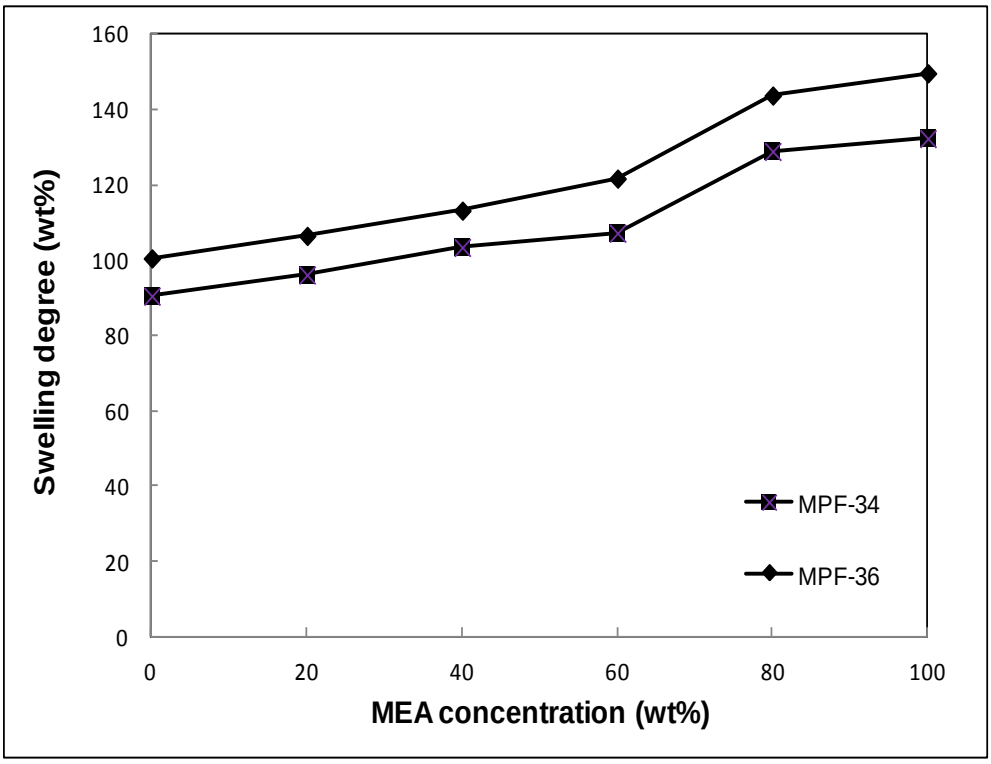

Figure 8 - The extent of swelling of the two membrane materials upon exposure to aqueous solutions of monoethanolamine (MEA)

Membrane samples were also left to soak in water, NaOH solution at pH approximately 12.4, 30 wt% MEA or pure MEA for up to five months. ATR-FTIR analysis was then used to evaluate any changes in membrane composition.

The results (Figure 9 - Figure 12) show that the MPF-34 membranes are stable at all operating conditions. They can sustain the high pH conditions and the membranes were not degraded by the MEA itself. The new peaks in Figure 11 and Figure 12, as indicated by the arrows, can be related to a residue of MEA solution within the membrane and on the membrane surface. From the literature, these peaks belong to hydrocarbon groups -C-H and -C-C, with IR wavenumber in the range of 2580 – 2960 cm^{-1} and 600 – 1500 cm^{-1} respectively. Results for the MPF-36 membranes were identical (data not shown).

Since the MPF-34 and MPF-36 are proprietary thin film composite nanofiltration membranes, a detailed discussion on the spectrum of each membrane material is not presented.

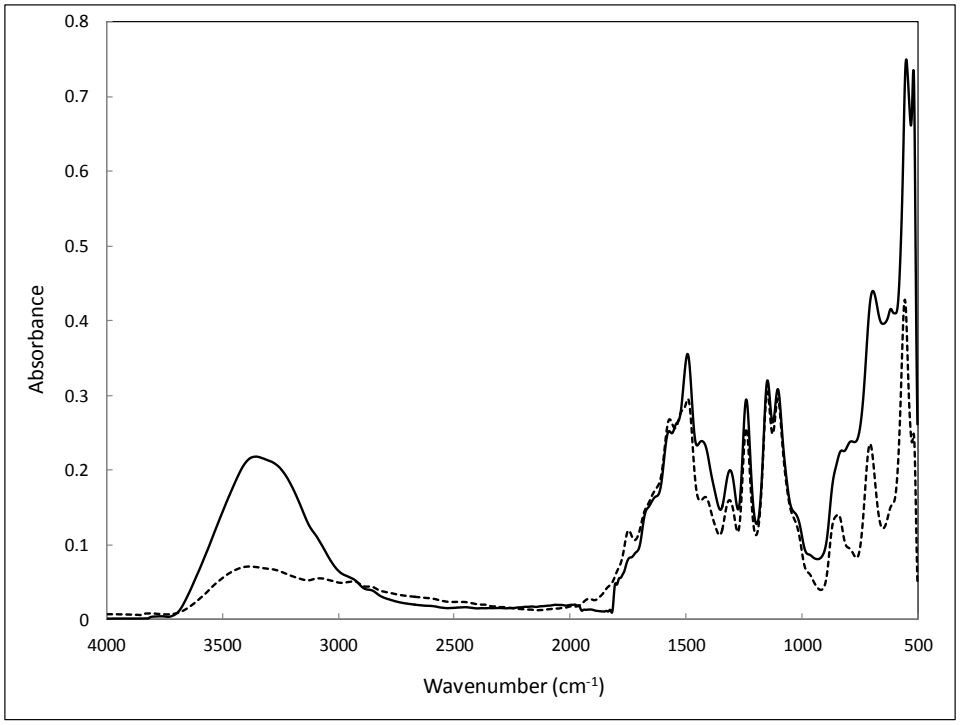

Figure 9 - The ATR-FTIR spectra for MPF-34 membranes in water (dashed line = dry membrane; solid line = soaked membrane)

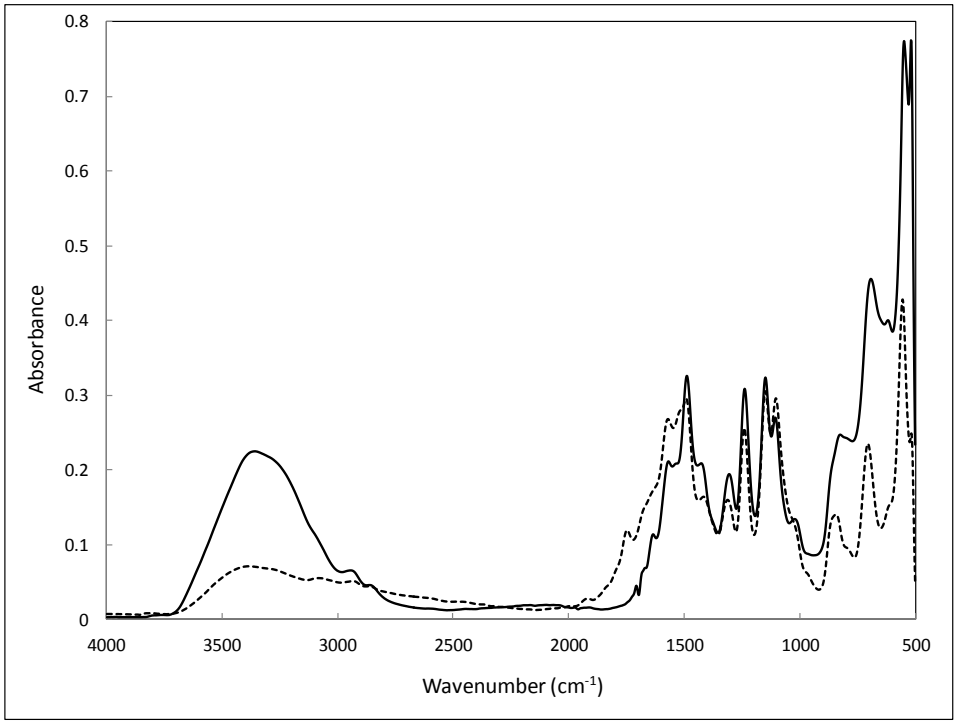

Figure 10 - The ATR-FTIR spectra for MPF-34 membranes in NaOH solution at pH approximately 12.4 (dashed line = dry membrane; solid line = soaked membrane)

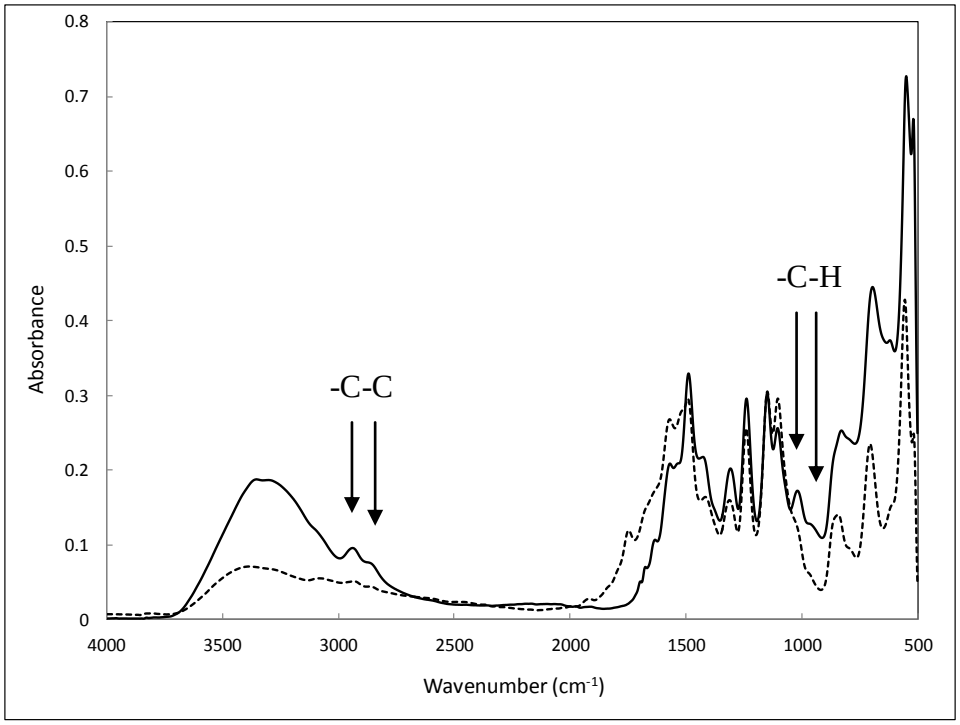

Figure 11 - The ATR-FTIR spectra for MPF-34 membranes in 30 wt% MEA (dashed line = dry membrane; solid line = soaked membrane)

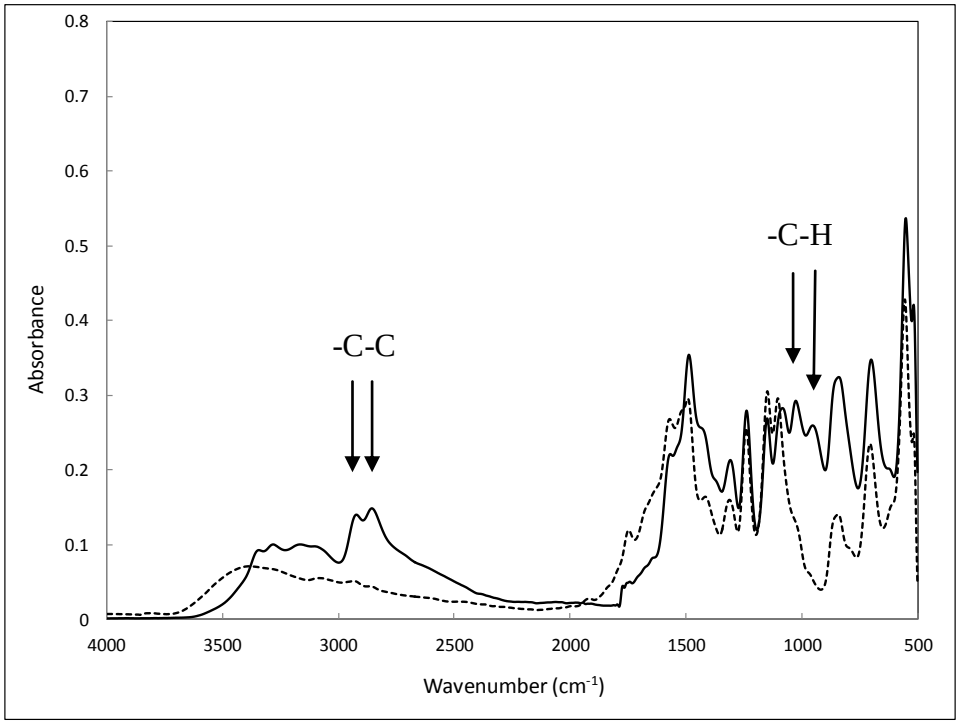

Figure 12 - The ATR-FTIR spectra for MPF-34 membranes in pure MEA solution (dashed line = dry membrane; solid line = soaked membrane)

Conclusions for NF

Nanofiltration using a Koch MPF-34 membrane has been shown to be an effective approach to concentrate the heat stable salts within an MEA solvent to facilitate downstream processing. The rejection of all heat stable anions evaluated exceeded 80 %, indicating a good retention of these species. Conversely, the MEA permeated the membrane, which would allow a clean solvent to be returned to the main process. It was shown that the nanofiltration process must operate on lean solvent, with MEA rejection increasing significantly as the loading increased, and the permeate flux falling.

This approach means that a downstream reclamation process, such as electrodialysis or thermal reclamation, can operate on a lower volume, more concentrated waste stream (the NF retentate), reducing costs. At the same time, the solvent circulating through the lean/rich solvent circuit can be maintained at lower impurity concentrations, leading to reduced energy costs from the lower viscosity and reduced maintenance costs due to lower levels of corrosion.

Electrodialysis (ED)

Electrodialysis (ED) is a membrane-based separation process in which an electrical potential difference is applied through a series of ion-exchange membrane in order to separate the ionic species in an aqueous solution [43, 44].

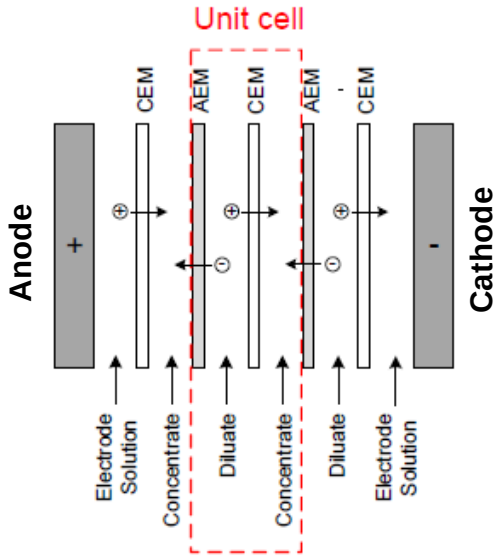

Figure 13 - The schematic diagram of the ED rig. Diluate = the depleted solution or the ionic solution losing the impurities. Concentrate = the concentrated solution or the ionic solution gaining the impurities.

Typically, the module is divided into a series of compartments (electrode, diluate and concentrate). The feed, with a high salt concentration, is directed to the diluate chambers, where under the influence of an electrical potential, ions are transferred into the concentrate chambers. Spacers are placed between the membranes, acting as a channel for the flow of the solution parallel to the membrane surface (Figure 13). The potential difference is generated by a DC power supply through two anodized metallic electrodes placed within the electrode chambers and the electrodes are typically platinized to reduce oxidation by strong bases and acids and corrosive gas.

In this project, the ion-exchange membranes used are limited to anion exchange membranes (AEM) and cation exchange membranes (CEM). AEM contains positively charged groups to allow anions to permeate and CEM contains negatively charged groups to allow cations to permeate through the membrane.

Under ideal conditions, the flux of ions between cells increases linearly as the stack voltage is increased, according to Ohm's Law (V=IR). Under these conditions, the current efficiency is 100 %; that is, the current is used entirely to move ions between cells. However, as the voltage increases, the phenomenon of concentration polarization can reduce current efficiency. In this scenario, the mass transfer of ions from the solution bulk to the membrane begins to become a significant resistance. The ion flux increase tails off as current increases until it reaches a limiting

current density (I_{lim}) (Figure 14) [45, 46]. At this point, the current density stabilizes. The point at which this stabilization occurs is a function of ionic concentration, fluid flowrates and the membrane resistance. However, as the voltage is increased further, the current density increases again. This is referred to as the overlimiting region and can be attributed to either electro-convection or to water splitting. Electro-convection refers to microscale fluid flows that develop within the depleted boundary layer due to electro-osmotic effects [47, 48]. Conversely, water splitting refers to the dissociation of water to provide ions that can carry the charge at the membrane surface [49]. Water splitting generally occurs more readily on the anion exchange membrane than the cation exchange membrane [50]. This latter phenomenon can also cause membrane degradation as the result of localized oxidation due to the formation of hydroxide and hydrogen ions. The presence of these ions may also cause scaling or precipitation of salts and organic matter on the membranes due to a sharp pH change close to the membrane surface [50].

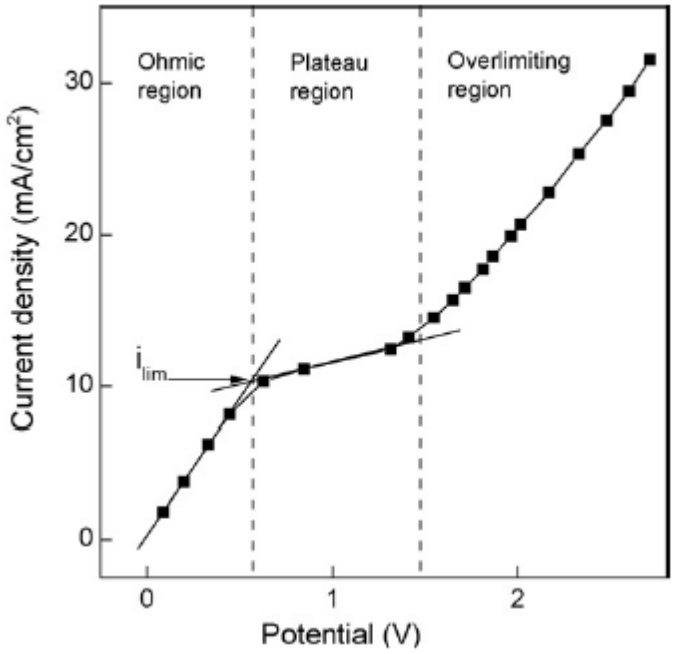

Figure 14 - An example of a current–voltage curve showing the relationship between the current density and the corresponding voltage drop over that membrane and its boundary layers (reproduced from [46]).

Membrane swelling due to solvent absorption and diffusion has also been shown to have a critical impact on the selectivity and permeation of mixed solvents. The absorption of solvent within the membrane may cause pore swelling and interfere with ion permselectivity [52]. Thus, it is important to choose ion-exchange membranes that are compatible with the working solutions in order to limit membrane degradation from the species present in solution, water splitting, or chlorine formation.

It is well established in the literature that ED should be conducted at low CO_2 loadings, to minimise loss of the charged carbamate ion from the diluate solution [9]. A further discussion of electrodialysis theory and applications can be found in our recently submitted paper [53].

Experimental details for ED

Materials for ED

Samples were prepared by mixing laboratory grade potassium oxalate monohydrate ($(COOK)_2.H_2O$, 98.5 %, Chem-Supply), potassium sulfate (K_2SO_4, 99 %, Ajax FineChem), potassium acetate (CH_3CO_2K, 99 %, Chem-Supply), potassium nitrate (KNO_3, 99 %, Chem-Supply), potassium carbonate (K_2CO_3, 99 %, Sigma-Aldrich), or potassium chloride (KCl, 99 %, Chem-Supply) with Reverse Osmosis (RO) water using a magnetic stirrer. For some samples, the background solution was a 30 wt% mixture of pure monoethanolamine (MEA, 99.5 %, Chem-Supply) and purified water (13.2 MΩ-cm). The concentration of the solutions used as the electrode, diluate and concentrate streams vary based on the purpose of the experiment. Further information on the working solution concentration is provided in the discussion.

The ion-exchange membranes were purchased from Membranes International Inc. (USA), Astom (Japan) and Fuma-Tech GmbH (Germany). All membranes were preconditioned to allow for membrane hydration and expansion. This was done by overnight immersion in a 5 wt% NaCl for Membranes International Inc. membranes and in 0.2 wt% KCl solution for Neosepta (Astom) and Fumasep (Fuma-Tech GmbH) membranes. Detailed information on the membrane properties is given in Table 4.

Table 4 - ED membrane properties

	Membranes International Inc. (MI)		Neosepta (Astom)		Fumasep (Fuma-Tech GmbH)			
	AEM	CEM	AEM	CEM	AEM		CEM	
Model	AMI - 7001	CMI - 7000	AHA	CMB	FAB (PEEK Reinforced)	FAA-3	FKB (PEEK Reinforced)	FKB
Thickness (mm)	0.45	0.45	0.22	0.21	0.1 – 0.13	0.05-0.055	0.08 – 0.11	0.09-0.11
Electrical resistance* (Ωcm^2)	< 40	< 30	4.1	4.5	<1	0.66	<4	<5
Total ion exchange capacity (meq/g)	1.3 ± 0.1	1.6 ± 0.1	-	-	>1.3	2.0	0.9 - 1.0	1.2 – 1.3
pH operating range	1 - 10	1 - 10			0 - 13	1 - 14	1 - 14	1 - 14
Base Polymer	Gel polystyrene cross linked with divinylbenzene functional group	Gel polystyrene cross linked with divinylbenzene	Polyethylene (50-70%)	Styrene, divinyl benzene copolymer	-		-	
Functional Groups	Quaternary ammonium	Sulfonic acid	trimethyl-ammonio-methyl (30-50%)	Sulfonic acid (45-60%)				

* measured in 0.5 M NaCl at 25°C

The ED experiments were conducted using an ED rig fitted with an MK-1 module from Ionics Incorporated (Massachussets, USA) or an FT-ED-40 module from Fuma-Tech GmbH (Germany). In these experiments, the module was set with two to eight pairs of cation and anion exchange membranes with alternating diluate and concentrate spacers. Detailed information for each module is presented in Table 5. The potential difference was generated by a DC power supply (Delta Elektronika, Netherlands, SM7020-D series) with an output voltage range of 0-70 V and output current range of 0-20 A.

Table 5 - ED cell properties

Module type	MK-1	FT-ED-40
Anode and Cathode	Platinized Titanium	Titanium-Iridium plasma coated
Effective area per membrane	232 cm^2	36 cm^2
Spacer type	Single and tortuous flow	Sheet flow, PVC/eCTFE spacer with Vexar screen
Flowpath length per spacer	348 cm	9 cm

Experimental procedures for ED

Three peristaltic pumps (Masterflex L/S digital drive 600 RPM with Masterflex L/S high performance pump head) were used to deliver the electrode, diluate and concentrate solutions to the ED module. The flow rate of the electrode solution was 1700 mL/min (850 ml/min per chamber) while the flow rate of the diluate and concentrate was kept equal and constant. A constant unidirectional current was applied to the module.

The experiments were conducted in two different modes: batch mode (Figure 15) and continuous mode (Figure 16). In batch mode, the electrode, diluate and concentrate solutions were re-circulated in three separate tanks. In continuous mode, only the electrode solution was re-circulated while the diluate and concentrate solutions were discharged after single use. The solution in each tank was mixed using a magnetic stirrer in order to obtain homogeneous solutions. Samples (approximately 25 – 50 mL each) from each stream were collected throughout the experiments for analysis.

The analytical methods were the same as the methods adopted in the nanofiltration experiments.

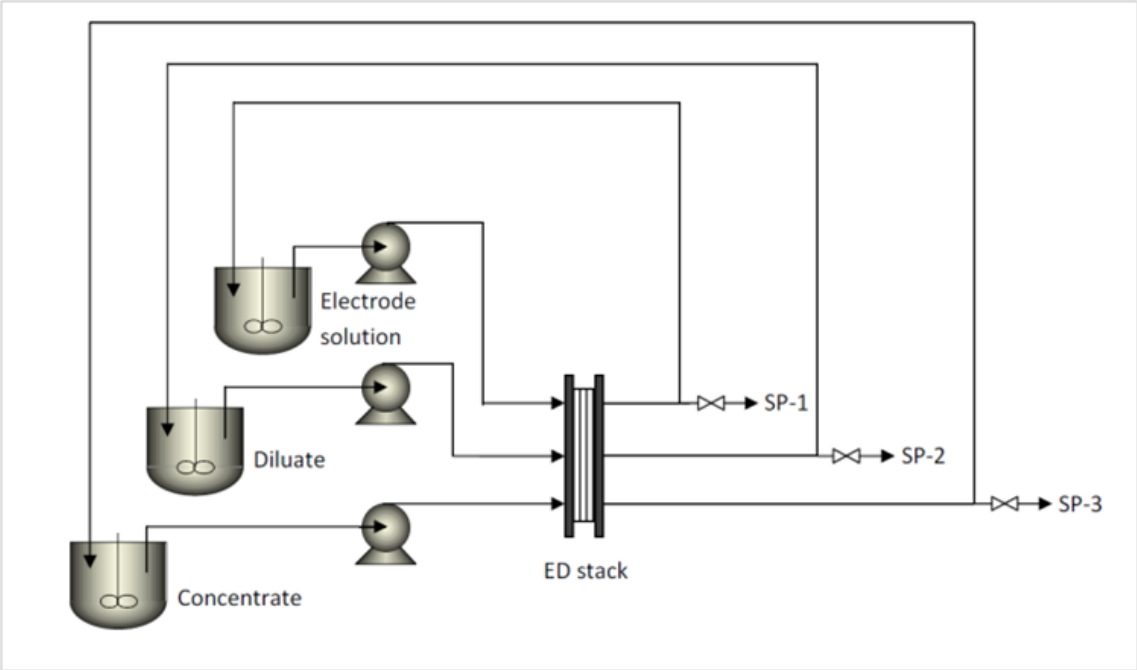

Figure 15 – A schematic diagram of batch mode electrodialysis (SP = sampling point)

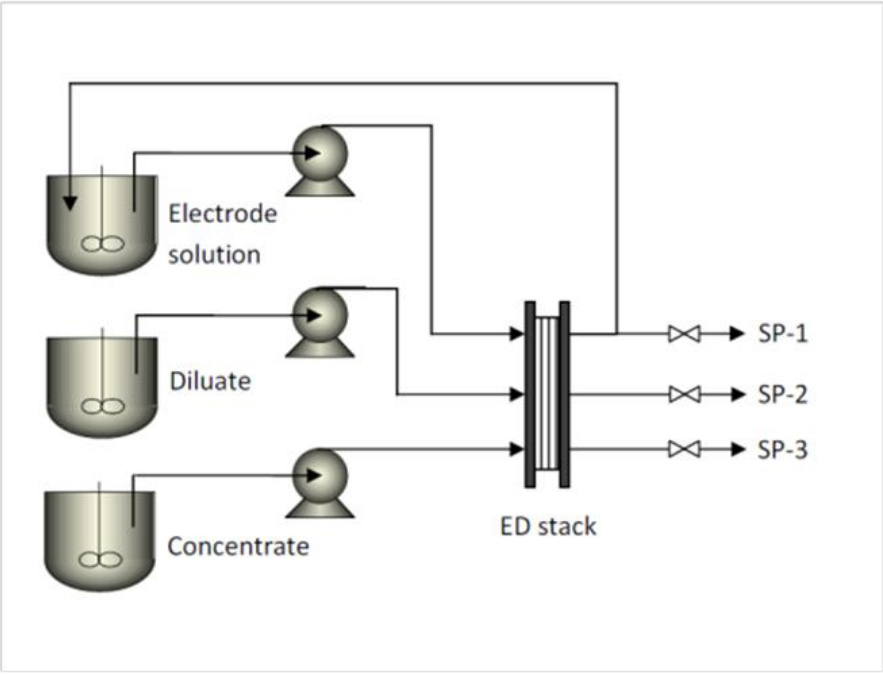

Figure 16 – A schematic diagram of continuous mode electrodialysis (SP = sampling point)

Results and discussion for ED

Concentration Polarisation and Membrane Resistance

Experiments were conducted in a continuous mode to determine the influence of diluate and concentrate flowrate, membrane type and concentration upon performance (Figure 17). At all conditions considered, operation occurs above the limiting current density, as indicated by the non-zero x-intercept of all curves.

A flowrate of at least 300 ml per minute per cell is required to eliminate the boundary layer resistance completely from 500 ppm aqueous solutions in the MI unit ((Figure 17a). Interestingly, this boundary layer resistance is less of an issue for the same concentration in 30 wt% MEA (Figure 17b). This reflects the greater electrical resistance of the MEA solution itself in these experiments. As the MEA solution is substantially organic, it is less able to carry charge and hence the solution resistance increases. This reduces the relative impact of the boundary layer.

A flowrate of at least 100 ml per minute per cell is required to eliminate the boundary layer resistance in the FT-ED-40 unit (Figure 17c) at similar concentrations in water. The resistance of the Fumasep FAB/FKB membrane stack is clearly lower than for the MI membranes. For example, for solutions of similar ionic strength (0.006-0.007 N), the MI unit provides around 21 A/m^2 at 10 V and 300 ml/min (giving a stack resistance of 4700 $\Omega.cm^2$, Figure 17a), while at the same voltage, use of 100 ml/min with the Fumatech membranes provides around 75 A/m^2 (a stack resistance of 1300 $\Omega.cm^2$ Figure 17c). This is consistent with the data in Table 5, which shows an order of magnitude difference in the membrane resistance when measured at 0.5 M NaCl.

The much larger resistance here, relative to the values in Table 5, results from the lower salt concentrations which will increase both solution and membrane resistance [46]. At higher concentrations, the stack resistance is much lower (200 $\Omega.cm^2$ at 10 V in 0.5 M KCl, Figure 17d). Under such conditions, the impact of concentration polarisation also reduces and flowrates as low as 25 ml/minute per cell can be used without a loss of performance in an aqueous solution.

It is readily apparent that it is important to maintain higher ionic concentrations in the feed/diluate stream in order to achieve an economic electrodialysis system.

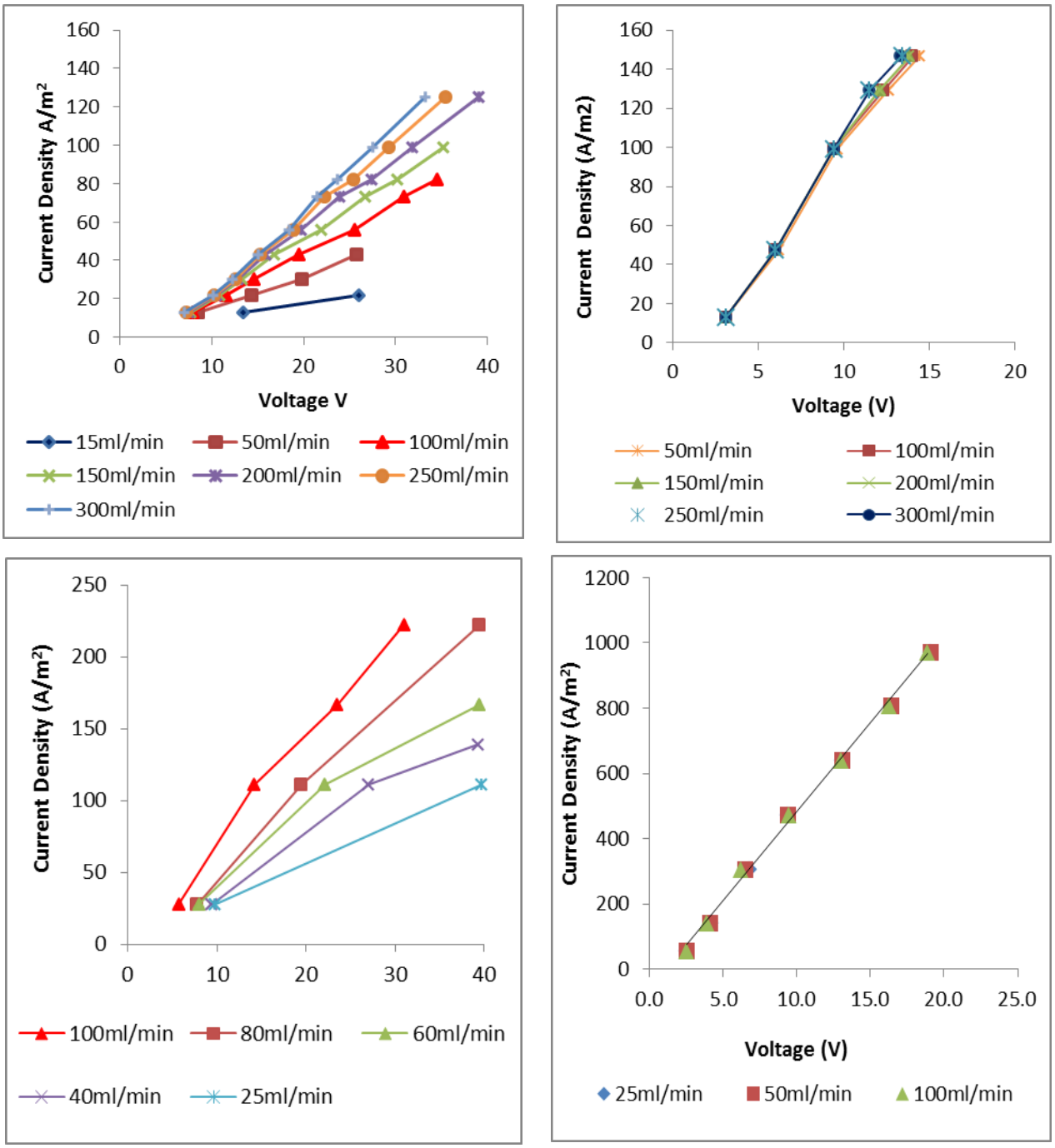

Figure 17 - Current density versus applied voltage as a function of the flowrate of diluate and concentrate per cell in two cell pair experiments (a) MI membranes in the MKD-1 cell, 500 ppm K_2SO_4 (0.006 N) in water both sides, (b) MI membranes in the MKD-1 cell, 500 ppm K_2SO_4 (0.006 N) in 30 wt% MEA both sides.(c) Fumasep FAB/FKB membranes in the FT-ED-40 unit , 500 ppm KCl (0.0067N) in water both sides (d) Fumasep FAB/FKB membranes in the FT-ED-40 unit, 0.5 N KCl (37 g/litre) in water both sides.

ED results for model solutions in water

To better understand the operation of the membranes and the ED cells, a number of experiments were conducted in pure water, without the complications of adding MEA.

In batch operation, the migration of the HSS anions from the diluate to the concentrate is reflected in both the change in the conductivity of the solutions and the measured anion concentration. As shown in Figure 18, in a batch operation 96 % of sulfate was observed to permeate from the diluate to the concentrate in 90 minutes, using the MI membranes in the MK-1 cell. There is a slight discrepancy between the amount of sulfate lost in the diluate and gained in the concentrate at any specific time. This is probably due to the absorption of some sulfate ions into the membrane during the early stage of the operation.

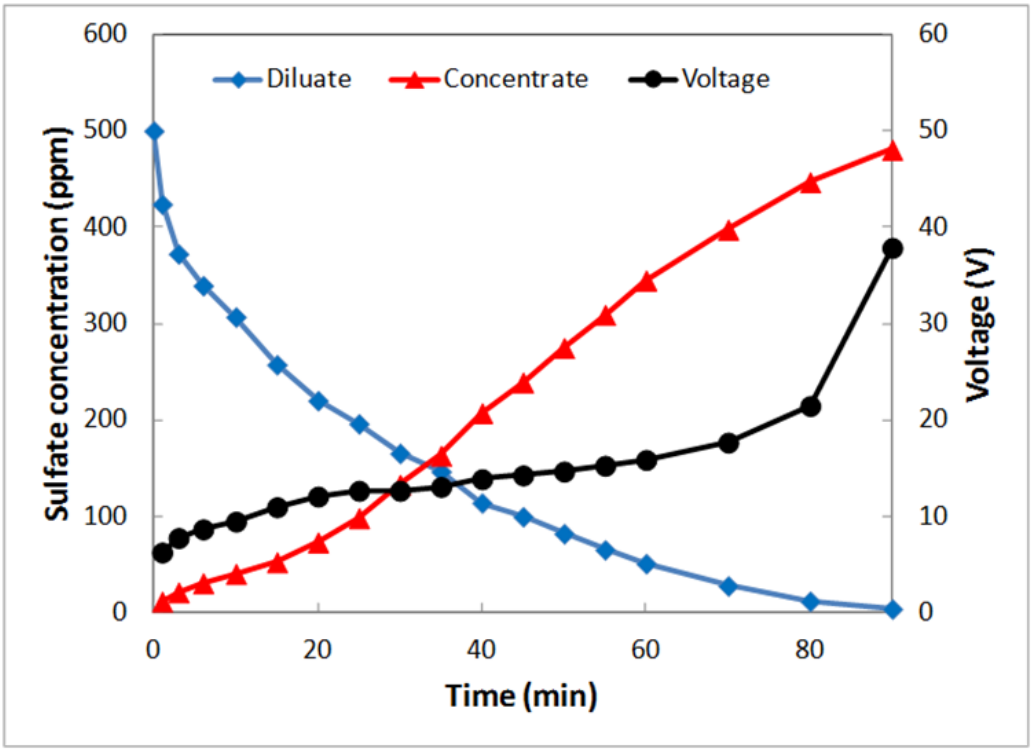

Figure 18 – Sulfate concentration and operating voltage as a function of time (Batch operation, MK-1 ED cell with MI membranes, 2 cell pairs, electrode = 5 wt% K_2CO_3, diluate = 500 ppm K_2SO_4, concentrate = 500 ppm K_2CO_3, current density = 21.6 A/m^2)

The effect of salt concentration on the operating voltage is also shown in Figure 18. The voltage increases as the sulfate permeates from the diluate to the concentrate. A significant increase in voltage can also be seen when the sulfate concentration falls below 50 ppm (90 % removal). This is because the resistance of the solution increases as the number of ions present in the diluate cell decreases as described above (Figures 17 c versus d), resulting in a higher voltage required for the transport of ions across the membranes. This is also apparent from Figure 19 which shows how the current efficiency falls as the diluate concentration falls. The current efficiency is the ratio of the current supplied to that used to actually move ions from cell to cell.

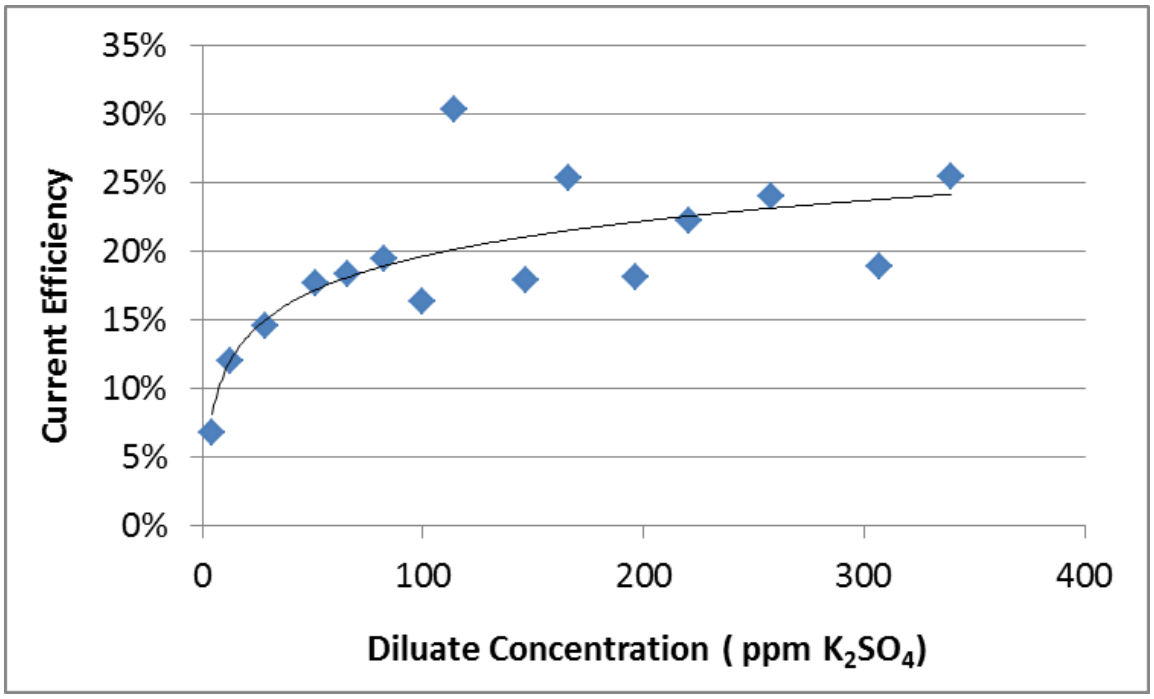

Figure 19 – The current efficiency falls and the stack resistance increases as the diluate concentration falls in batch operation (MK-1 cell with MI membranes, 2 cell pairs, electrode = 5 wt% K_2CO_3, diluate = 500 ppm K_2SO_4, concentrate = 500 ppm K2CO3, current density = 21.6 A/m^2)

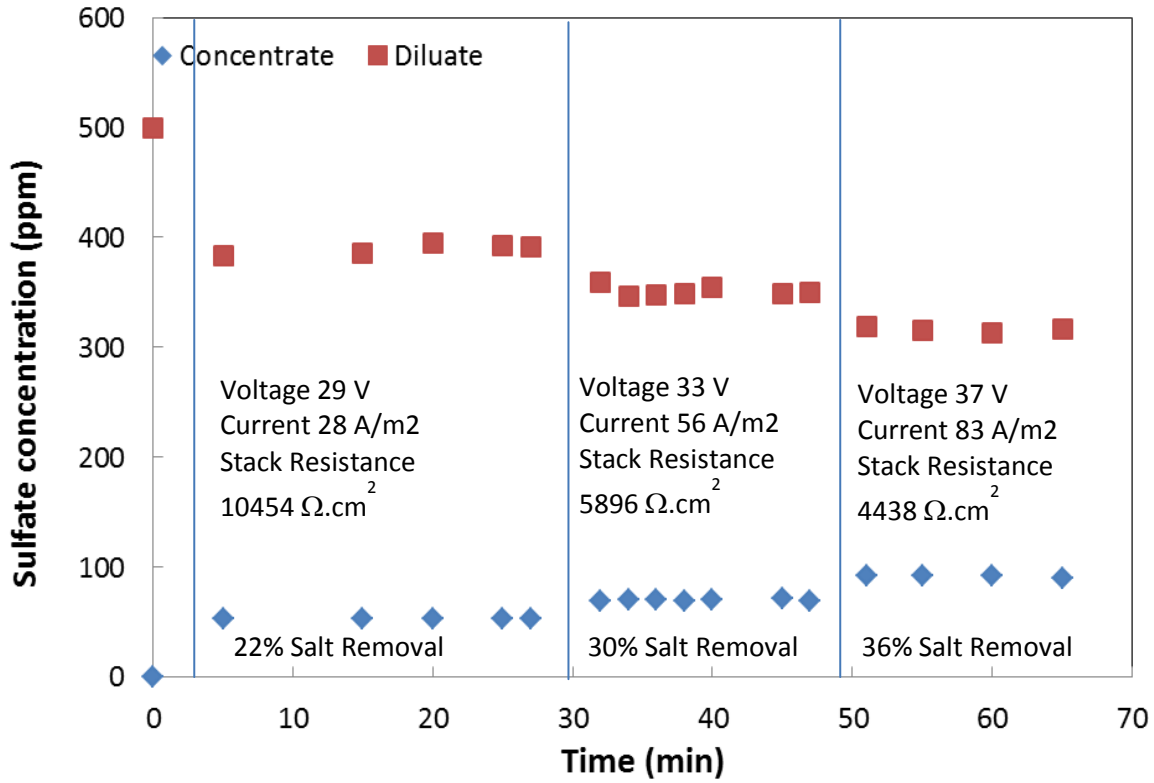

Figure 20 – The effect of current density on sulfate concentration in continuous operation (FT-40 ED cell with Fumasep FAB/FKB membranes, 2 cell pairs, electrode = 5 wt% K_2CO_3, diluate = 500 ppm K_2SO_4, concentrate = water)

In continuous operation, the extent of ion removal is limited by the residence time within the membrane stack. As shown in Figure 20, the extent of sulfate removal increases with an increase in the current density, from 22% at 28 A/m^2 to 36% at 83 A/m^2. However, given the residence time within the unit is only 1.1 seconds this is still a good result. In industrial practice, greater removal rates would be achieved by increasing both the membrane area and the residence time within the unit.

The extent of salt removal for a range of anions was also investigated at higher salt concentrations (Figure 21). Once again the extent of removal increases with the applied current density. The removal of sulfate and nitrate ions is considerably more efficient than that of oxalate and acetate, as indicated by the current efficiency. The reason for these changes is not clear, but may relate to the hydrophobicity (or hydrophilicity) of the ions. Acetate and oxalate are less polar (as indicated by the strength of their acids) and hence may move more slowly through the highly hydrophilic membrane material.

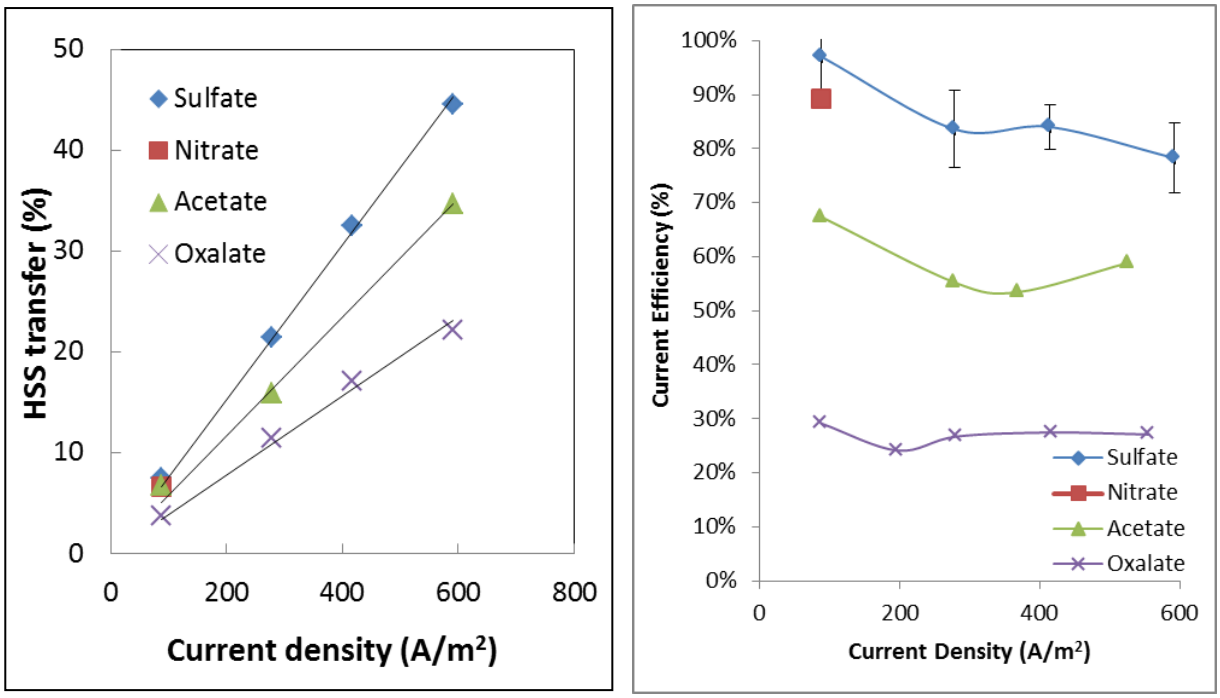

Figure 21 – The extent of salt removal for different HSS at different current densities (continuous operation, FT-40 ED cell, Fumasep FAB/FKB membranes 2 cell pairs, electrode = 5 wt% K_2SO_4, diluate = concentrate = 20 g/litre potassium sulfate, nitrate, acetate and oxalate).

ED results for MEA based model solutions

An important design criteria for an ED process in this application will be the rate of loss of MEA across the membranes. This needs to be minimized to ensure that solvent loss is small. This loss was relatively easy to determine in the MK-1 unit, where the membrane area is relatively large so concentration changes are significant (Figure 22).

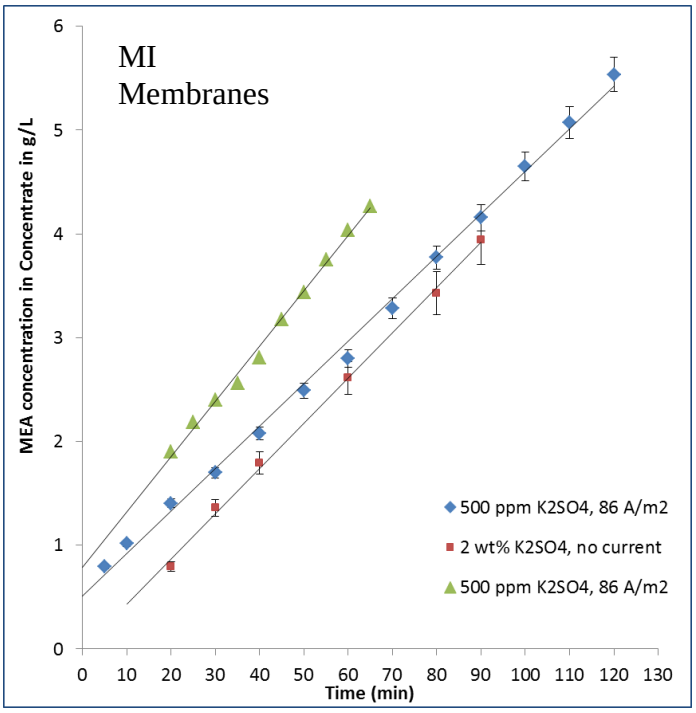

Figure 22 – The transport of MEA solution through MI membranes under a range of operating conditions (Batch operation, MK-1 ED cell, 2 cell pairs, electrode = 5 wt% K_2CO_3, flowrate per cell 150 ml/minute). Two runs are conducted with 500 ppm K_2SO_4 in 30 wt% (300 g/litre) MEA at 86 A/m^2. The third run was at 5 wt% K_2SO_4 in 30 wt% MEA, but no voltage was applied across the stack.

Conversely, the FT-ED-40 unit is smaller, so transfer rates are lower and the experimental error is thus greater. In these runs, there is also clearly an initial period where MEA is sorbing into the membrane material, so that true transfer does not occur until 20 or 30 minutes into the experiment. The MEA loss estimated from this technique is summarized in Table 7. It is apparent that the MEA loss is lowest across the MI membranes, as might be expected for these thicker membranes, which also have lower ion transfer rates. The loss from the PEEK reinforced Fumasep FAB/FKB and Neosepta membranes is comparable, while that from the Fumasep FAA-3/FKB is higher, reflecting the very delicate nature of these unreinforced membranes.

Table 6 – Calculated Average MEA Loss from a 30 wt% solution into the concentrate.

Membrane type	Membranes International	Fumasep FAB/FKB (PEEK Reinforced)	Fumasep FAA-3/FKB	Neosepta
Loss (g MEA/m^2.s)	0.054 ± 0.002	0.19 ± 0.09	0.82	0.17 ± 0.07

The rate of ion transfer is strongly affected by the presence of MEA in the feed (diluate) stream (Figure 23a). This predominantly reflects the fact that in a 30 wt% MEA solution, only 70 % of the solution is water and thus able to carry the ions. This is supported by conductivity measurements during experiments. For example, in the feed solution of 5 g/litre K_2SO_4, the conductivity falls from 5.2 to 2.75 mS/cm when the solvent is changed from water to 30 wt% MEA. This lack of conductivity affects both the amount transferred and the current efficiency (Figure 23b), which ultimately impacts the energy demand.

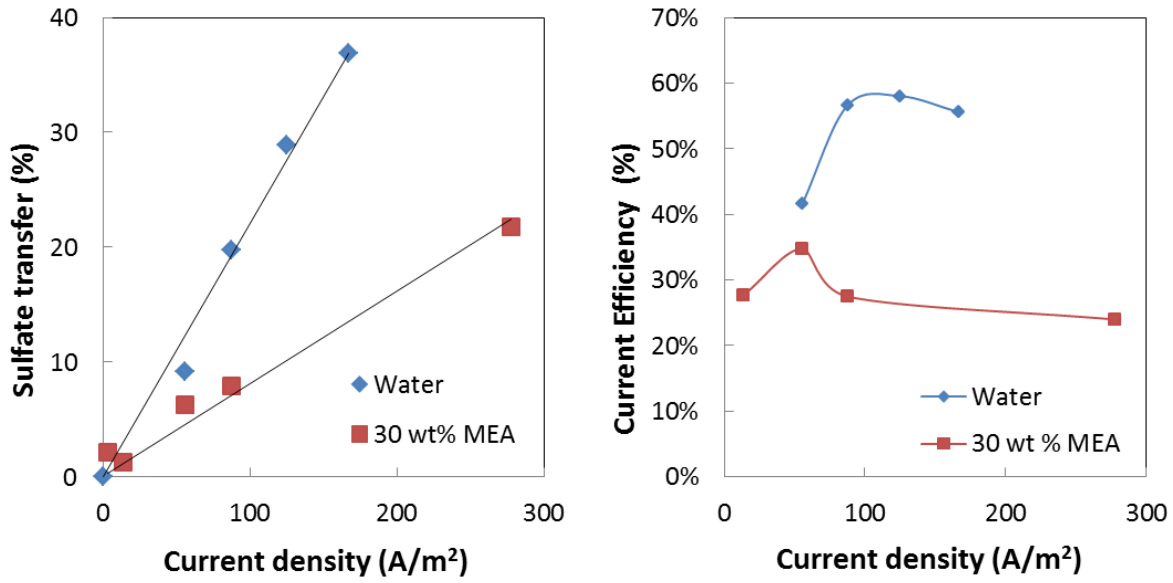

Figure 23 – The effect of MEA on sulfate removal and current efficiency at different current densities (continuous operation, FT-40 ED cell with Fumasep FAB/FKB membranes, 2 cell pairs, electrode = 5 wt% K_2SO_4, diluate = 5 g/litre ppm K_2SO_4 in water or in 30 wt% MEA, concentrate = 2 g/L KCl)

The transfer rate under continuous flow conditions has also been evaluated for both sulfate and nitrate as a function of the current density (Figure 24). Consistent with the results presented in Figure 21 for these salts in water the transfer of sulfate is slightly better than that of nitrate. Both transfer rates increase with the current density, although the current efficiency falls (data not shown).

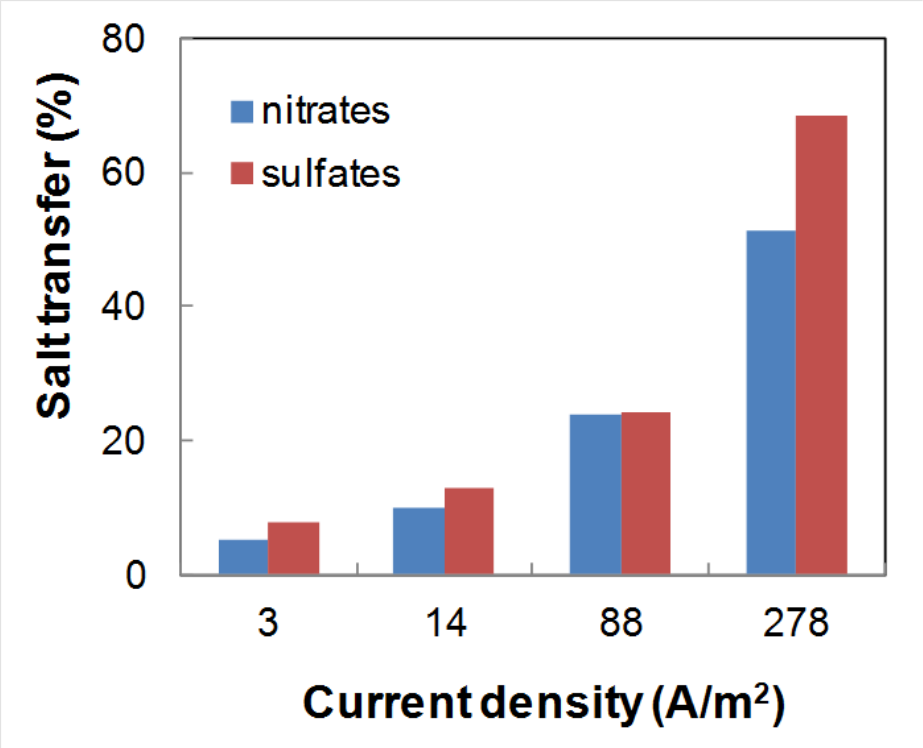

Figure 24 – The extent of salt removal for different HSS at different current densities with the presence of 30 wt% MEA in the diluate stream (Continuous operation, FT-40 ED cell with Neosepta Membranes, 2 cell pairs, electrode = 5 wt% K_2SO_4, diluate = 500 ppm K_2SO_4 or KNO_3 in 30 wt% MEA, concentrate = 2 g/L KCl)

The final investigation focused on the relative performance of different ion exchange membranes within an MEA system. For this purpose, identical experiments were conducted using Fumasep and Neosepta membranes with both 500ppm and a 5000ppm K_2SO_4 in 30 wt% MEA (Figure 25). These results suggest that the Neosepta membranes provide slightly better current efficiency and lower power consumption for a given current. It is difficult to include a comparison of the MI membranes under the same circumstances, due to the different designs of the ED cells. However, the single point available under identical conditions shown in Figure 25 suggests that their performance is the worst of the three membrane types. At this point (86 A/m^2, 500 ppm K_2SO_4 feed), the stack resistance of the MI system is higher, which results in the slightly greater power consumption. This is consistent with the data presented for a water-based system in Figure 17, where again the MI stack had a greater resistance than the Fumasep stack.

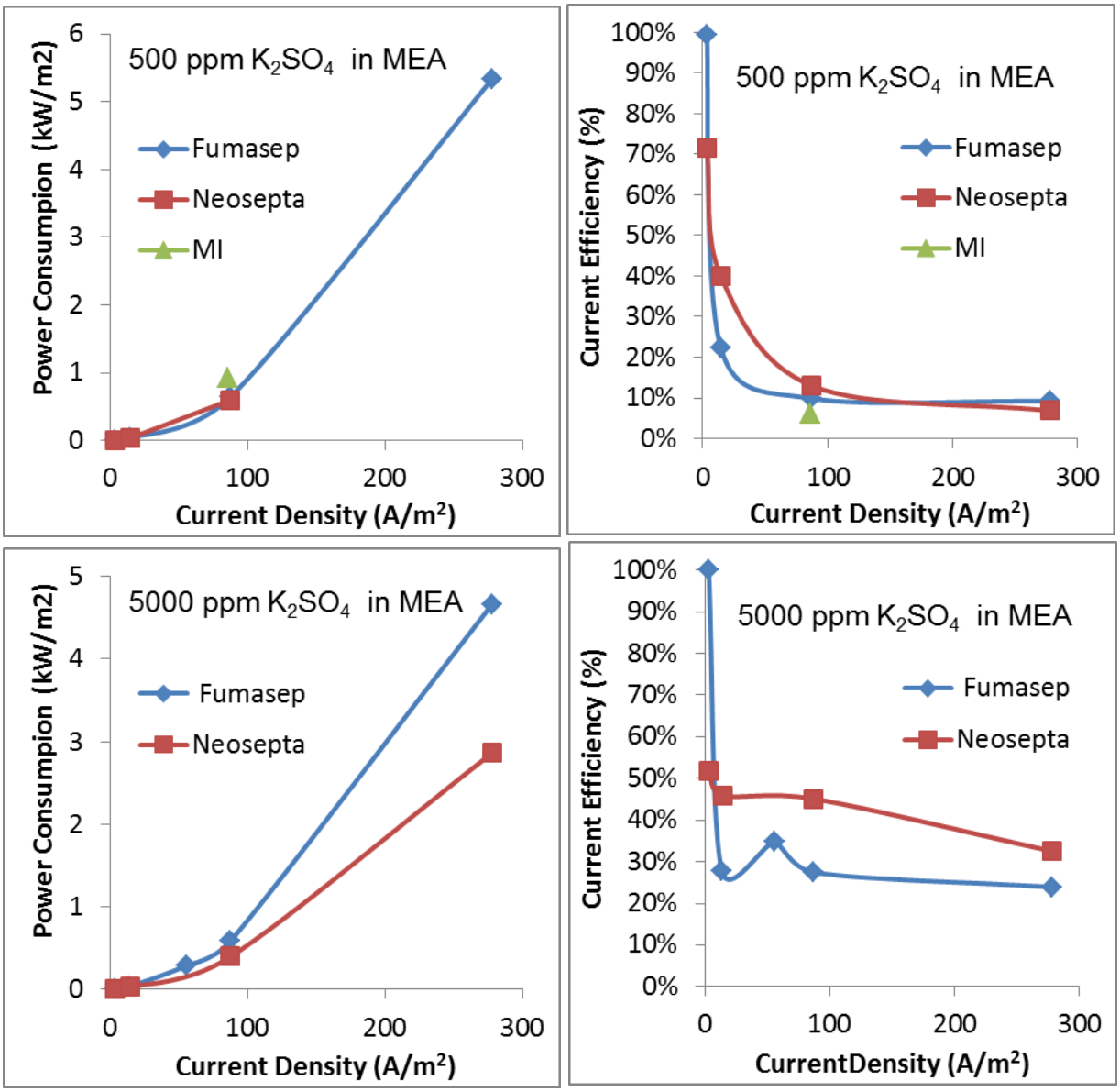

Figure 25 – Current efficiency and power consumption for ED operation using Fumasep FAB/FKB, Neosepta and MI membranes (continuous operation, 2 cell pairs, electrode = 5 wt% K_2SO_4,) (a) diluate = 500 ppm K_2SO_4 in 30 wt% MEA (b) diluate = 5000 ppm K_2SO_4 in 30 wt% MEA

ED membrane stability

The compatibility of the three commercial ion exchange membrane for MEA based operation was also evaluated based on the swelling and the change in the membrane composition over time.

The results from the swelling test indicate that all membranes investigated are stable in MEA solutions for a concentration up to 40 wt% (Figure 26). While there is only a slight increase in the swelling degree of the membranes from Membrane International (MI) and Astom (Neosepta), Fuma-Tech (Fumasep) membranes swell the most. In fact, the Fumasep AEM (FAA-3) membrane was dissolved upon immersion in > 60 wt% MEA for 24 hours. Thus, the swelling degree data for a concentration > 60 wt% can not be presented. The immersion in high

concentration MEA solution also changed the shape of the Fumasep CEM membrane. The membrane was visually observed to expand in a lateral direction at MEA concentration higher than 60 wt%.

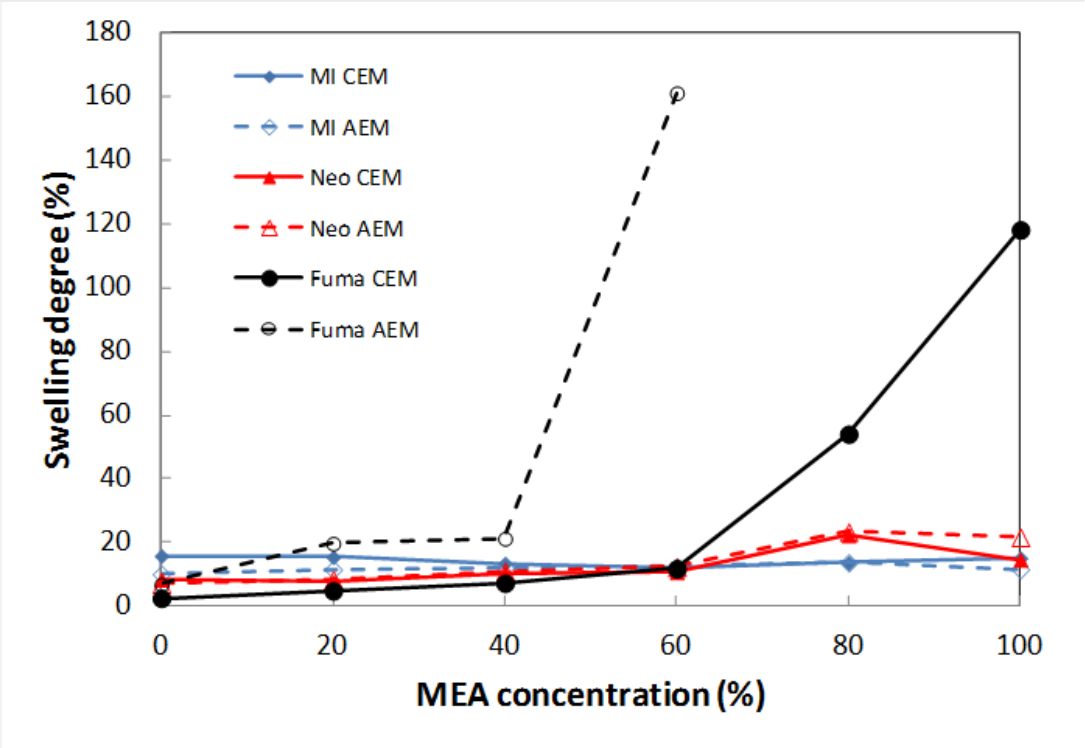

Figure 26 – The extent of swelling of commercial ion-exchange membranes upon exposure to aqueous solutions of MEA (MI = membranes from Membrane International Inc., Neo = Neosepta membranes, Fuma = Fumasep membranes (FAA-3, FKB), CEM = cation exchange membranes, AEM = anion exchange membranes)

In terms of the membrane chemistry, the results from the ATR-FTIR measurements are presented in Figure 27 - Figure 32. There is no evidence that the ion exchange membranes are degraded upon soaking in 30 wt% MEA solution for up to 4.5 months. However, both cation and anion exchange membranes from Membrane International Inc. were observed to strongly discolour upon immersion in MEA solution. The colour was observed to change from white (AEM) / brown (CEM) to black at all MEA concentration investigated. At MEA concentration > 80 wt%, the surface of both membranes peeled off readily.

The exact composition of the membrane materials is beyond the scope of this study hence detailed discussion on the functional groups of each membrane is not presented.

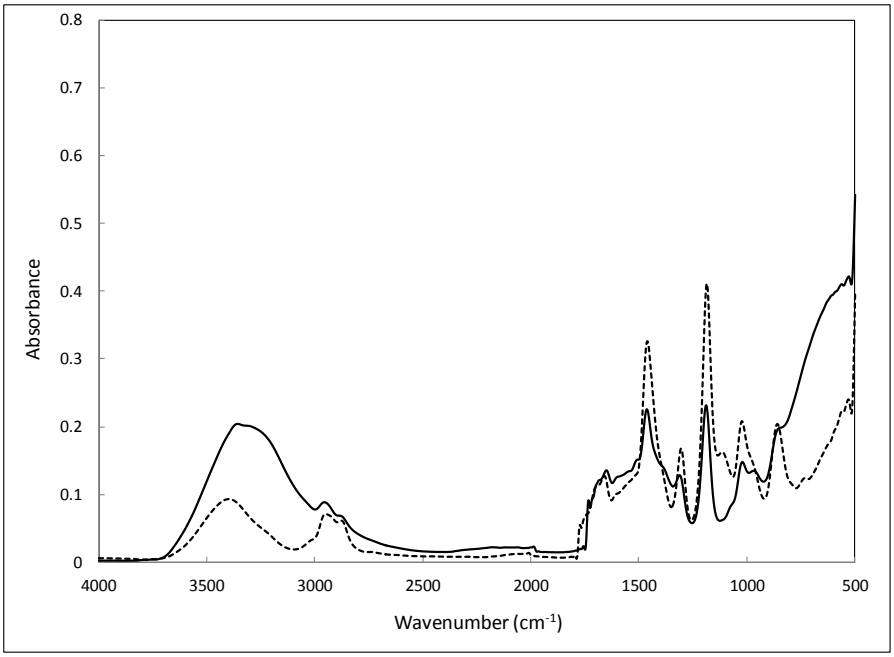

Figure 27 – The ATR-FTIR spectra for Fumasep anion exchange membrane in 30 wt% MEA solution (dashed line = dry membrane; solid line = soaked membrane)

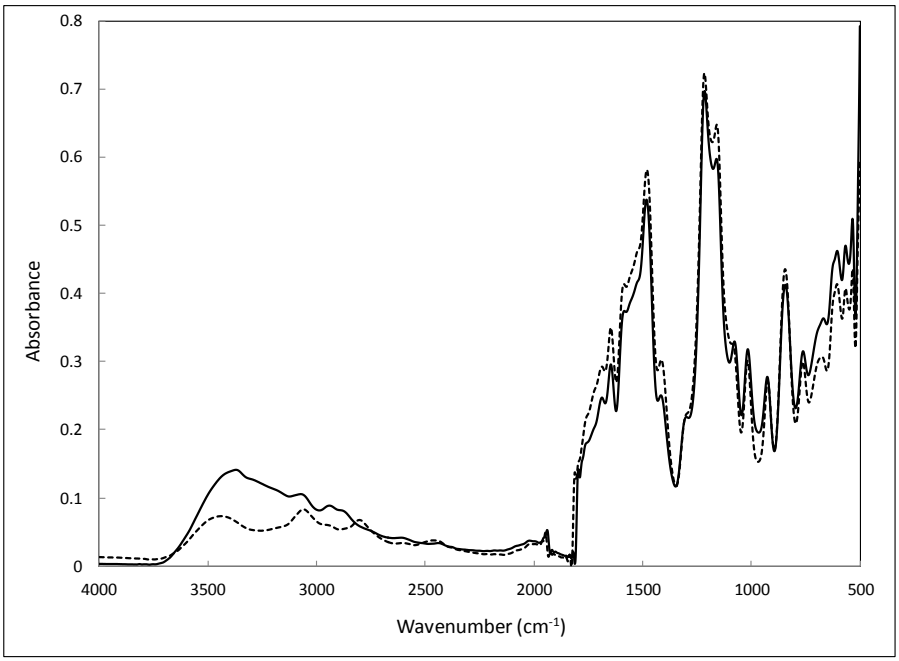

Figure 28 – The ATR-FTIR spectra for Fumasep cation exchange membrane in 30 wt% MEA solution (dashed line = dry membrane; solid line = soaked membrane)

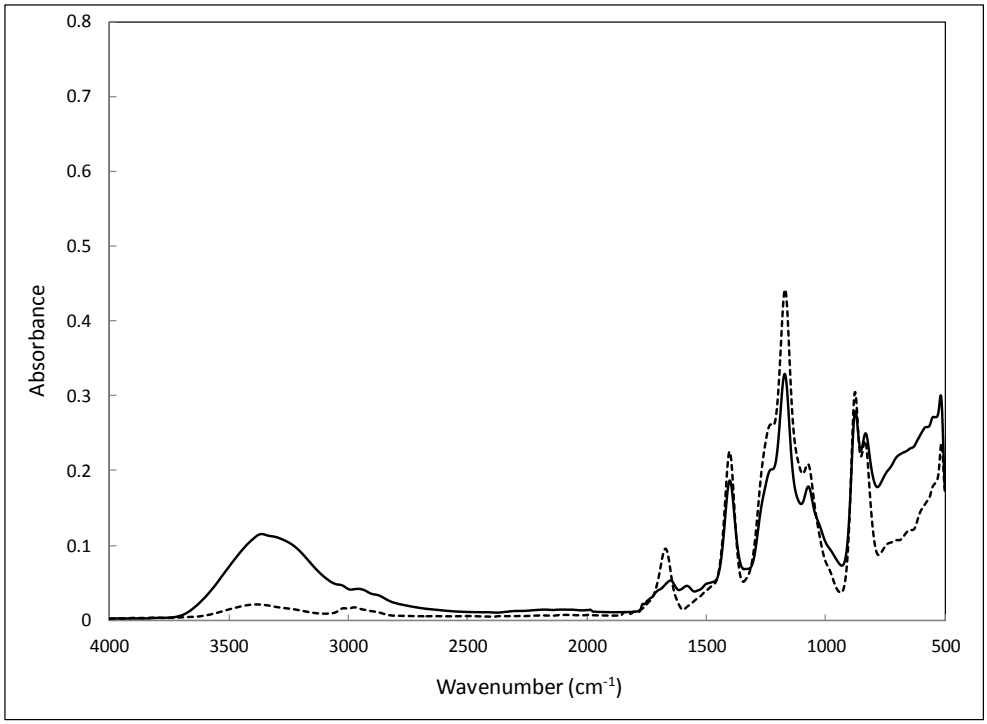

Figure 29 – The ATR-FTIR spectra for Membrane International Inc. anion exchange membrane in 30 wt% MEA solution (dashed line = dry membrane; solid line = soaked membrane)

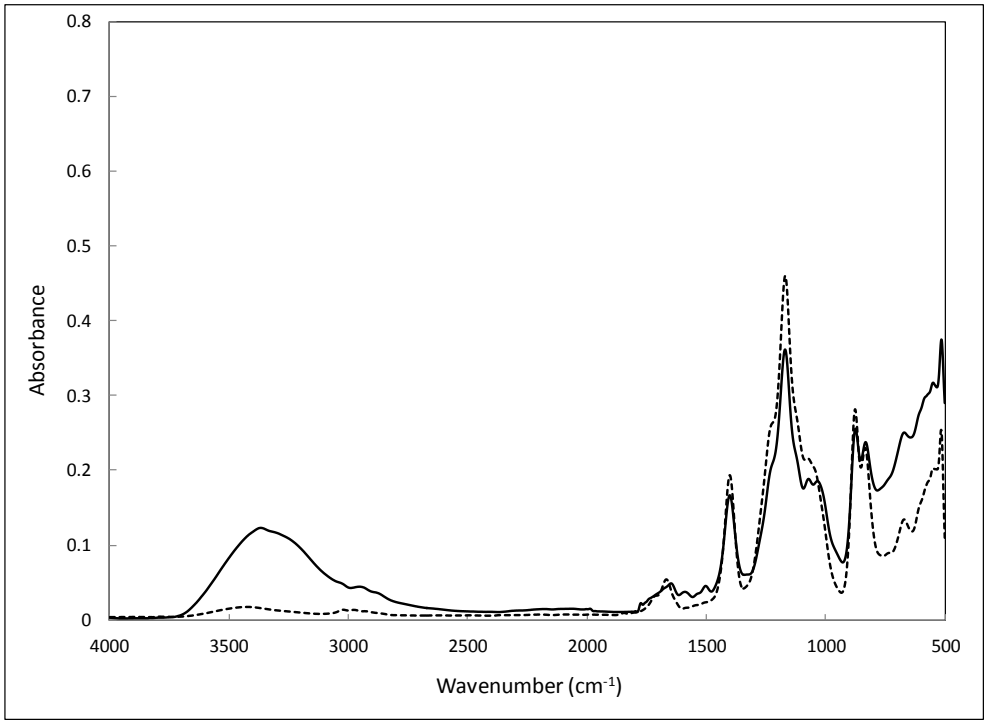

Figure 30 – The ATR-FTIR spectra for Membrane International Inc. cation exchange membrane in 30 wt% MEA solution (dashed line = dry membrane; solid line = soaked membrane)

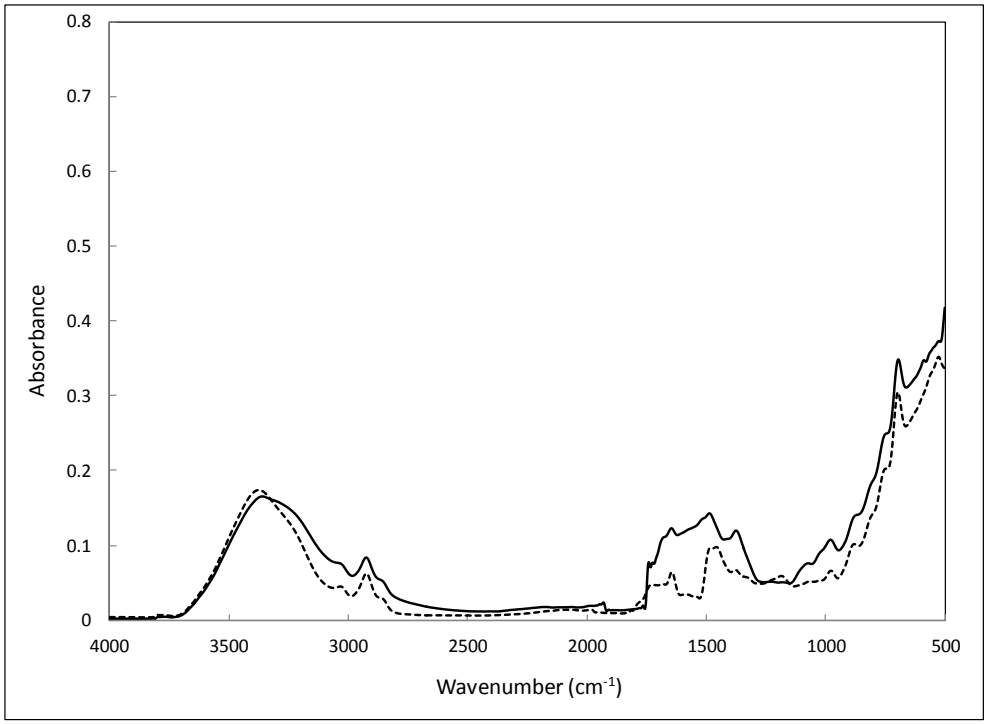

Figure 31 – The ATR-FTIR spectra for Neosepta anion exchange membrane in 30 wt% MEA solution (dashed line = dry membrane; solid line = soaked membrane)

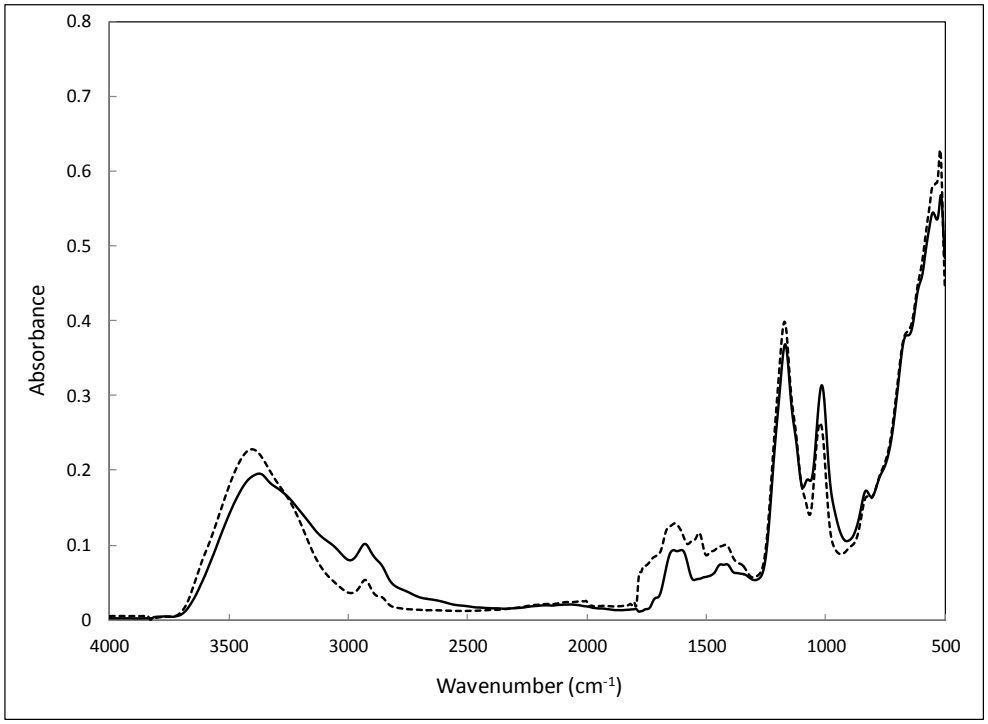

Figure 32 – The ATR-FTIR spectra for Neosepta cation exchange membrane in 30 wt% MEA solution (dashed line = dry membrane; solid line = soaked membrane)

Conclusions for ED

This study has shown that electrodialysis is an effective approach to promote ion transfer across a series of ion-selective membranes. In batch operation, 96 % sulfate removal was achieved. It was shown that maintaining the ion concentration in the concentrate (the depleted solution) is essential for minimising the overall energy consumption. Additionally, a higher salt removal could be achieved by increasing the operating current density.

The efficiency of the operation decreased in the presence of 30 wt% MEA. This was reflected in lower current efficiencies and higher energy demand. Commercial ion-exchange membranes from Membranes International Inc. (AMI-7001 and CMI-7000), Astom (Neosepta AHA and CMB) and Fumatech GmbH (Fumasep FAA-3, FAB and FKB) all proved suitable for the MEA electrodialysis operation, although the Fumatech FAA-3 membrane dissolved at high (60 wt%) MEA concentrations. The ATR-FTIR study showed that the membrane chemistry did not change upon soaking in a 30 wt% MEA solution for a period of up to 4.5 months.

Of the membranes tested, the Neosepta combination appear to be the best choice for further testing, as they are stable in concentrated MEA solutions and appear to provide slightly better current efficiency and power consumption.

Nanofiltration and electrodialysis of industrial aged amine solvent

Experimental details for industrial solvent

Sample preparation

Aged MEA solvents: MEA50+ and MEA1800+ (supplied by CSIRO) were used in the study. The samples were sourced from the Post-combustion Carbon Capture (PCC) pilot plant at Loy-Yang power station. The number represents the number of hours that the solvent had been used to capture CO_2 in the PCC plant, hence the MEA50+ and MEA 1800+ had been used for 50 and 1800 hours respectively (2 days and 10 weeks, if continuous operation). The solvents were a clear brown solution of relatively low viscosity upon delivery (see Table 8). As a comparison, the viscosity of a pure 25 wt% MEA solution is expected to be 2.12 mPa.s [42].

Both NF and ED processes operate best at low CO_2 loadings [9], where the carbamate concentrations are minimized. While the loading of the MEA 1800+ was reasonably low at delivery (0.12, see Table 8), the loading of the MEA 50+ was 0.31, too high for effective ED or NF. Hence, it was necessary to reduce the loading by simple boiling of the solution prior to use. In industrial practice, the solution for reclamation would be taken from the cool, lean solvent circuit, where the loading should be less than 0.15.

Thermal boiling of MEA50+ solvent was carried out in batches using a 2 L round bottom flask with a condenser at the top. The flask was filled with 1.5 L solvent and heated to a temperature of 110 – 120 °C at atmospheric pressure. Cold tap water (single pass) was used as the condensing agent to reduce the loss of MEA through evaporation. Small samples (approx. 5 mL) were taken periodically to monitor the loss of MEA and CO_2 from the solution. The boiling was continued until the measured CO_2 loading was less than 0.15 mol CO_2/mol MEA (Table 7). The boiled solution was then cooled to room temperature and mixed with the solutions from the other batches prior to use.

Similarly, by changing the pH of the solution above the pKa value of MEA, the amount of protonated amine present is minimized. This minimizes both the loss of amine across the ED membrane and maximizes the passage of amine across the NF membrane. This neutralization step is a standard pre-treatment process in commercial ED and thermal reclamation processes, as discussed further in our review paper [9]. Thus, both MEA50+ and MEA1800+ were neutralised prior to use by adding 10 M NaOH until the pH was approximately 12.4. The amount of NaOH added was approximately 380 mL for 3 L MEA50+ solvent and 463 mL for 3 L MEA1800+ solvent. This equates to an average of 1.4 mol NaOH (56 g) of NaOH per litre of aged solvent. Neutralisation reduced the MEA concentration in both samples by approximately 10 %, due to the additional volume of NaOH solution added. The addition of NaOH also increases the solution conductivity by approximately 2 mS/cm due to the presence of more ionic species in the sample.

The neutralization step resulted in the precipitation of a significant mass of material, presumably heat stable salts, which could be visually observed to settle at the bottom of the sample containers. These salts were then removed from the solvent by microfiltration through a flat sheet 0.2 µm PTFE membrane with polypropylene non-woven support layer (Sterlitech Corporation (USA)). The Sepa CF Membrane Element cell used for nanofiltration experiments was used for this microfiltration step, with a transmembrane pressure of 300 kPa. After filtration, the membrane was clearly fouled with a gel like, clear deposit. There were some patches of brown, indicative of metal content, but this was not extensive.

Table 7 – The physical and chemical properties of aged MEA solvents before and after the pre-treatment steps

	MEA 50+			MEA 1800+	
	Upon Delivery	After boiling	After boiling, neutralisation	Upon Delivery	After neutralisation
Conductivity (mS/cm)	12.7		14.5	13.5	15.3
Density (kg/m^3)	1029		-	1076	-
Viscosity (mPa.s)	2.4		2.4	4.3	4.3
pH	10.3		12.45	10.64	12.3
MEA concentration (wt%)	22.7[1] or 21.9[2]	23.5[2]	19.1[1]	27.7[1] or 26.6[2]	24.0[1]
CO_2 loading (mol CO_2/mol MEA)	0.31		0.13	0.12	0.14

(Measurements were conducted at approximately 23 °C)
[1] Measured using Metrohom autotitrator
[2] Measured by CSIRO

Experimental procedures for industrial solvent

A Koch MPF-34 membrane was used in all nanofiltration experiments with the industrial solvent. The full experimental procedure for this experiment is presented in the previous section – Nanofiltration.

Electrodialysis of the industrial solvent used the FT-ED-40 module (Table 5) from Fuma-TechGmbH, Germany (Table 4). The Neosepta (AHA, CMB) ion-exchange membranes (Astom, Japan) were selected due to the combination of membrane stability and low electrical resistance.

All ED experiments were conducted in batch mode (Figure 15) with two cell pairs. The flow rate of the electrode solution was 1700 mL/min while the flow rate of the diluate and concentrate was kept equal and constant at 200 mL/min (100 ml/minute per cell). The full experimental procedure for this experiment is presented in the section related to Electrodialysis.

Analytical methods for industrial solvent

The measurement of pH, conductivity, MEA concentration, CO_2 loading and membrane composition (ATR-FTIR) is the same as the previous section (Nanofiltration). Additional measurements are given below.

Solution viscosity was measured using a Canon Fenske viscometer and solution density was measured using a 25 mL density bottle. A second measurement of MEA concentration was conducted by CSIRO, whereby 0.25 g sample was diluted with water (to a volume of 50 mL) followed by an addition of 2 mL (1 M) HCl. The final mixture was then titrated against 0.5 M NaOH until the equivalence point was reached. The volume of NaOH added was used to

determine the amount of HCl that is not reacting with amine, which was then used to calculate the MEA concentration of the sample.

The concentration of sulfate and nitrate was quantified using ion chromatography (Dionex ICS-1000, AS14 column) with a mixture of 2.7 mM carbonate and 1 mM bicarbonate as the eluent. A number of elements (K, Na, S, Fe, Al, As, B, Ba, Ca, Cr, Cu, Mg, Mn, Mo, Ni, P, Pb, Si, Sr, Ti, V, Zn) were quantified using an Inductively Coupled Plasma – Optical Emission Spectroscopy (Varian 720 ICP-OES). Both IC and ICP analysis could only be performed when the MEA concentration was low (concentrate samples), due to the incompatibility of the analytical instruments with organic materials. It was not possible to determine the ionic species in the feed or diluate samples directly.

A qualitative analysis to identify the presence of MEA and other organic species in a solution was conducted using Nuclear Magnetic Resonance (NMR) spectroscopy. 1H and 13C NMR studies were conducted using an Agilent DD2 500 MHz NMR with D_2O used as an internal standard. The spectrum of the analysed sample was compared with the spectrum of pure MEA (99.5 %, Chem-Supply) solution.

Results and discussion for industrial solvent

NF and MF/NF results for MEA50+ and MEA1800+

Initially, a nanofiltration experiment was conducted on as-received MEA50+ solvent. It was observed from the experiment that the solvent could not permeate through the NF membrane even at a trans-membrane pressure of 3000 kPa. This is due to the high CO_2 loading of the as-received MEA50+ (0.31 mol CO_2/mol MEA), which means that there was a significant amount of carbamate anions present in the feed solution. Given that the iso-electric point of Koch MPF-34 membrane is at pH 3 – 4 [38], the membrane was negatively charged upon exposure to the feed solution (pH = 10.3). A strong surface charge repulsion then occurred between the negatively charged membrane and carbamate anions. This resulted in an osmotic pressure difference that is greater than the trans-membrane pressure and zero permeate flux. The subsequent NF experiments were then limited to the use of MEA50+ and MEA1800+ solvents after thermal boiling and neutralisation.

The NF results for the MEA50+ and MEA1800+ solvents (after thermal boiling and neutralisation) are shown in Figure 33. Compared to the data for 30 wt% MEA model solution (lab-prepared using a mixture of pure MEA and purified water), the permeate flux for MEA50+ reduces by up to a factor of 10 while the permeate flux for MEA1800+ solvent reduces more significantly up to a factor of 60. The loss of performance reflects the increasing osmotic pressure imposed by the feed solution. This osmotic pressure arises from the fact that the CO_2 loading of the solution is not zero. The osmotic pressure is given by the x-intercept of the flux versus pressure curve, suggesting a value of 920 kPa. This corresponds to a concentration of charged ions of 0.4 mol/litre, which can readily be explained by the CO_2 loading (see Figures 4 and 6). The use of microfiltration upstream of nanofiltration here has little effect on the final results, indicating that membrane fouling is not the cause of the loss in flux.

The rejection of charged salts also falls under these conditions, again reflecting the relatively high CO_2 loading (Figure 7) but also the relatively high concentrations of heat stable salts. It was not

possible to determine the rejection of any particular salt directly, due to the complexity of the aged solution. However, the solution conductivity can give an indirect measure of the rejection of charged species (inclusive of carbamates, protonated amines and heat stable anions). As shown in Table 9, the total rejection of charged species is less than 20 %. This is inadequate for a commercial process. To be viable, the CO_2 loading would need to be reduced further.

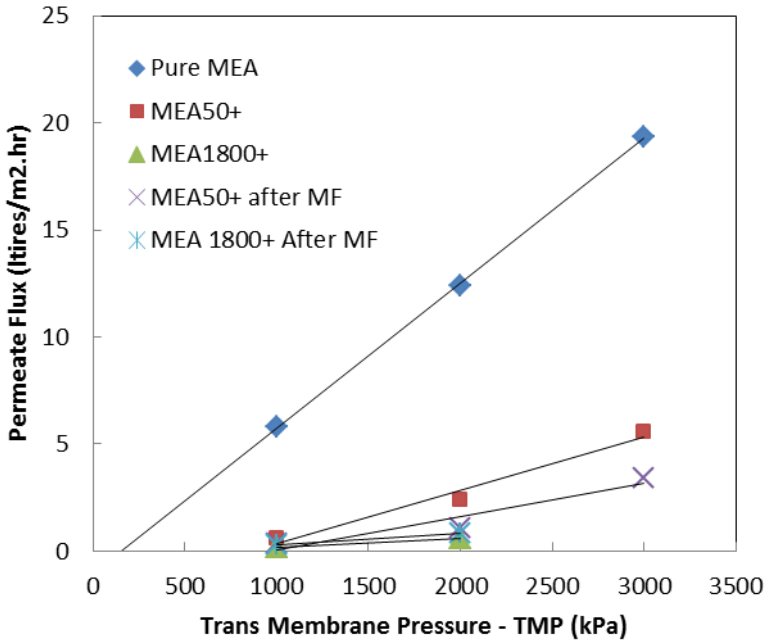

Figure 33 – The permeate flux for 30 wt% MEA (model solution), MEA50+ (after thermal boiling and neutralisation) and MEA1800+ (after neutralisation) at different pressures using MPF-34 membrane

Table 8 – The conductivity of the feed and permeate solution in the NF MEA50+ experiment and the estimated total rejection of charged species.

	Conductivity (mS/cm)	Rejection (%)
Feed solution	15.0	
Permeate (at 1000 kPa)	12.2	19
Permeate (at 2000 kPa)	12.4	17
Permeate (at 3000 kPa)	12.9	14

MF/ED results for MEA50+ and MEA 1800+

The MF/ED result for the MEA50+ sample is presented in Figure 34. As shown by the change in the conductivity of the diluate and concentrate, there is indeed a significant ion transport from the diluate to the concentrate solution. The conductivity of the electrode solution also reduces over time, indicating the transport of ions from the electrode solution to the concentrate. The ion transport is also reflected by the gradual change in the colour of the concentrate solution into the colour of the feed solution (aged MEA50+). This colour is believed to arise chiefly from heat stable salts and oxidation products, as a pure MEA solution is colourless.

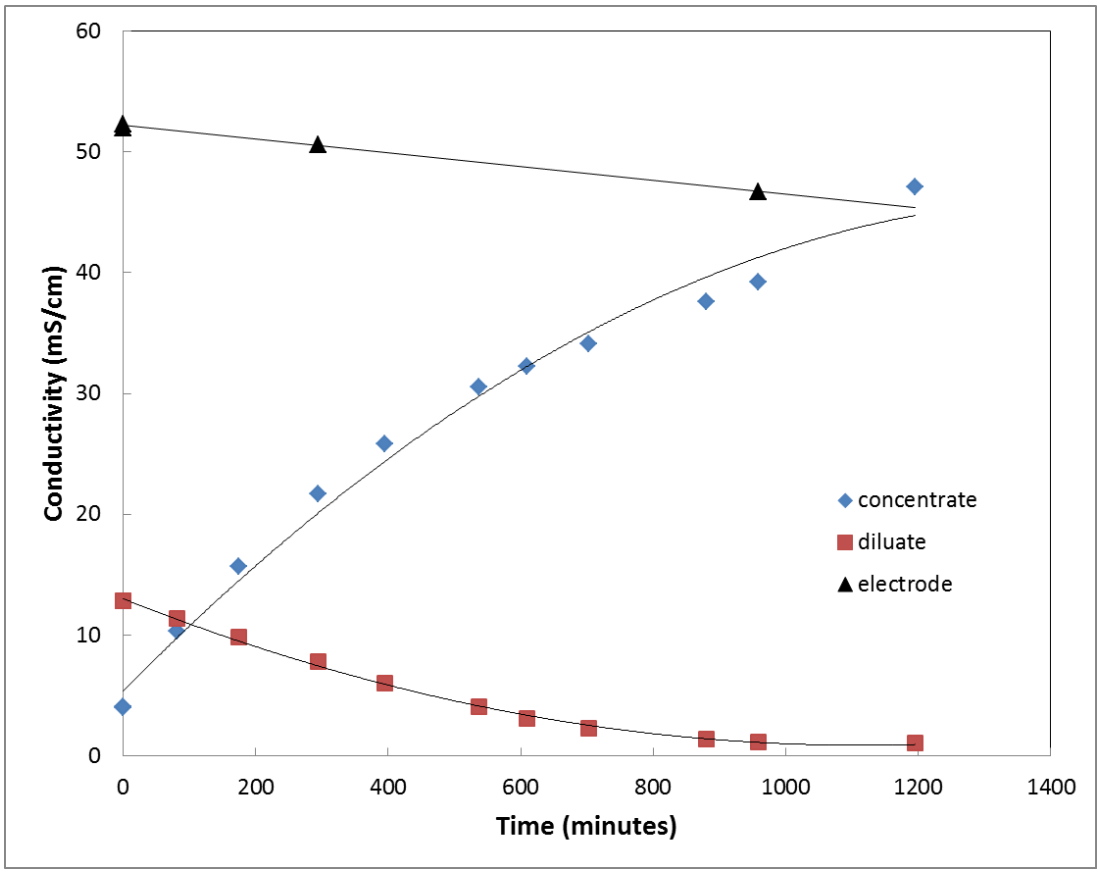

Figure 34 – The change in the diluate, concentrate and electrode solution conductivity over time (diluate = MEA50+ after thermal boiling, neutralisation and microfiltration; current density = 278 A/m^2, Neosepta membranes in two cell pairs)

The significant increase in the concentrate conductivity relative to the diluate conductivity reflects the significant organic content of the MEA 50+. Since an organic solution has a lower conductance compared to an inorganic solution, the nominal value of the solution conductivity does not represent the amount of ions in the system. In other words, although the amount of ions lost from the diluate is equal to the amount of ions gained in the concentrate, the change in the nominal value of their conductivity will not be the same. The conductivity of the diluate is reduced from 12.8 to 1.03 mS/cm in 1195 minutes of operation, representing 92 % removal of all charged species. The use of a larger membrane area relative to the flow through the cell would reduce this timeframe.

A similar experiment was conducted on MEA1800+. As shown by the results in Figure 35, there is a similar trend on the change in the diluate, concentrate and electrode solution conductivity. In this case, the experiment was stopped after 800 minutes, limiting the total salt transfer (as indicated by conductivity) to 46 %. It is expected that a longer experimental time or a greater membrane area would result in further ion transport from the diluate to the concentrate. The ion transport is also reflected again by the gradual change in the colour of the concentrate and electrode solution.

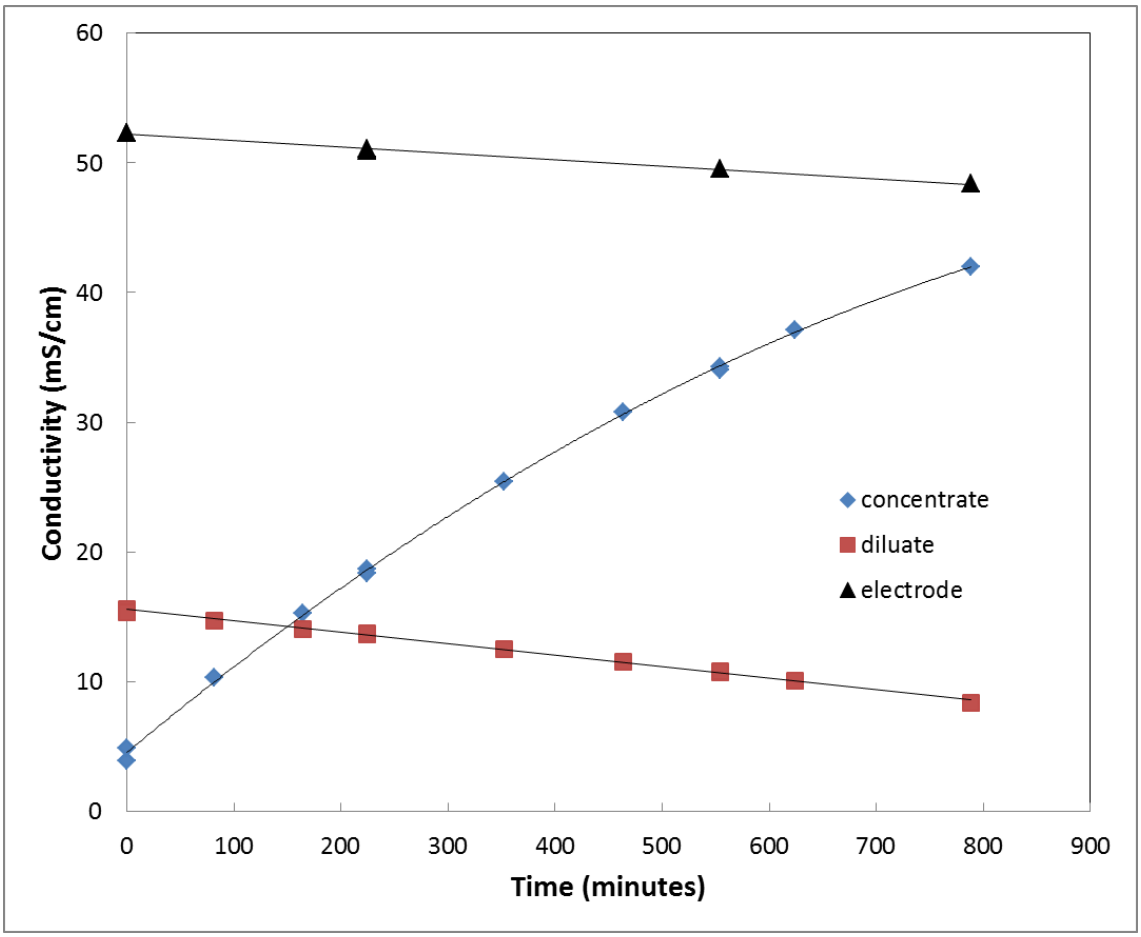

Figure 35 – The change in the diluate, concentrate and electrode solution conductivity over time (diluate = MEA1800+ after thermal boiling, neutralisation and microfiltration; current density = 278 A/m^2)

The pH of all the working solutions was also monitored (
Figure 36). Even before the application of an electrical potential, the pH of the concentrate and electrode solution increased. Within 20 minutes, the pH of both solutions had increased from 4 - 8 to around 10. This finding reflects the high mobility of OH^- and H^+ ions which means that they permeate the membranes readily without the need for a driving electrical potential. Once the voltage was applied, the concentrate pH continued to drift up slowly, with the diluate solution drifting down, reflecting continuing transfer of OH^- ions from the diluate to the concentrate.

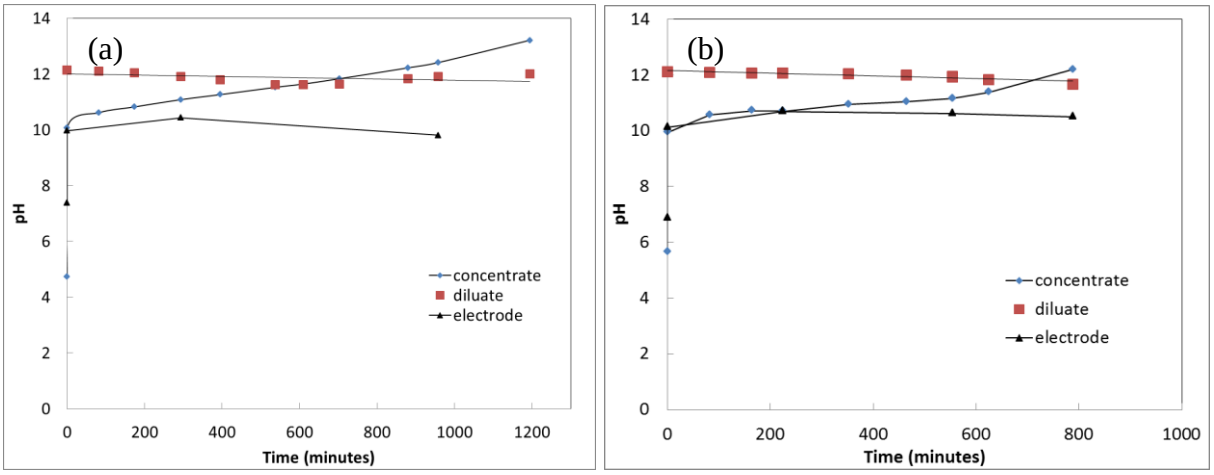

Figure 36 – pH of the diluate, concentrate and electrode solution as a function of time (a) MEA50+ (b) MEA 1800+ after thermal boiling, neutralisation and microfiltration; current density = 278 A/m^2)

An elemental analysis to quantify the extent of ion transport across the membranes was obtained using ICP analysis. In this experiment, the analysis was limited to the concentrate samples due to the limitation in the analysis method. In general, the amount of all investigated elements in the concentrate tank increases over time. The amount of each element at the end of the experiment is given in Table 9.

Table 9 – Concentrate composition in the MF/ED MEA50+ experiment

(sample was collected at the end of the experiment)

	Concentrate Composition		*mg/litre (ppm)*	*Predicted Feed Composition (after neutralization)*		*mg/litre (ppm)*
ICP Analysis	Sodium	Na	4,300	Sodium	Na	4,300
	Potassium	K	14,400	Potassium	K	~0
	Calcium	Ca	2.7	Calcium	Ca	2.7
	Iron	Fe	0.61	Iron	Fe	0.61
	Sulphur	S	204	Sulphate	SO_4	612
	Zinc	Zn	0.97	Zinc	Zn	0.97
	Arsenic	As	0.03	Arsenic	As	0.03
	Molybdenum	Mo	0.19	Molybdenum	Mo	0.19
	Boron	B	0.83	Boron	B	0.83
	Barium	Ba	0.04	Barium	Ba	0.04
	Chromium	Cr	0.06	Chromium	Cr	0.06
	Vanadium	V	0.01	Vanadium	V	0.01
	Silicon	Si	16.9	Silicon	Si	16.9
	Selenium	Se	0.03	Selenium	Se	0.03
	Ruthenium	Ru	1.1	Ruthenium	Ru	1.1
	Phosphorus	P	0.34	Phosphorus	P	0.34
	Nickel	Ni	0.38	Nickel	Ni	0.38
	Manganese	Mn	0.05	Manganese	Mn	0.05
	Magnesium	Mg	0.02	Magnesium	Mg	0.02
Ion Chromatography	Sulphate	SO_4	509			
	Nitrate	NO_3	62	Nitrate	NO_3	62

Given that the concentrate solution was originally 2000 mg/L KCl, the presence of other elements clearly shows ion transport from the diluate to the concentrate. In fact, given the concentrate and diluate volumes are identical it is possible to use this data to estimate the approximate feed concentration to the ED unit. For the MEA 50+, as 92 % of the conductivity was depleted from the diluate, we assume that the feed composition is essentially identical to the concentrate, but the original potassium in the concentrate is subtracted, as is leakage from the electrode solution. The sulfur content is also converted to an equivalent sulphate concentration (Table 9).

It is important to understand that this is the predicted feed composition after neutralization. However, the neutralization step itself involved the addition of 30 g/litre of sodium ions. The fact that only 4.3 g/litre of sodium appears in the concentrate, suggests that a significant quantity of sodium has precipitated as solid salts during the neutralization process. It is likely that these precipitated salts were a mixture of sodium sulphate, sulphite, nitrate and nitrite salts. Hence the feed solution prior to neutralization contained significantly greater quantities of sulfur and nitrogen based anions.

For the MEA1800+ solution, similar assumptions are made, but the concentrate concentrations are doubled, as only around half of the conductivity was depleted from the diluate (Table 10). We hope to confirm these estimates of the feed composition through an analysis to be completed by CSIRO.

Table 10 – Concentrate composition in the MF/ED MEA1800+ experiment (sample was collected at the end of the experiment)

	Concentrate Composition		*mg/litre (ppm)*	*Predicted Feed Composition (after neutralization)*		*mg/litre (ppm)*
	Sodium	*Na*	9,896	Sodium	Na	9,896
	Potassium	K	10,483	Potassium	K	~0
	Calcium	Ca	2.5	Calcium	Ca	5
	Iron	Fe	8.1	Iron	Fe	16.2
	Sulphur	S	492	Sulphate	SO_4	2,952
	Zinc	Zn	0.29	Zinc	Zn	0.58
ICP Analysis	Arsenic	As	0.06	Arsenic	As	0.12
	Molybdenum	Mo	0.21	Molybdenum	Mo	0.42
	Boron	B	0.09	Boron	B	0.18
	Barium	Ba	0.04	Barium	Ba	0.08
	Chromium	Cr	0.02	Chromium	Cr	0.04
	Vanadium	V	0.1	Vanadium	V	0.2
	Silicon	Si	2.0	Silicon	Si	4.0
	Selenium	Sr	0.05	Selenium	Se	0.1
	Ruthenium	Pb	0.03	Ruthenium	Ru	0.06
	Phosphorus	P	0.41	Phosphorus	P	0.82
	Nickel	Ni	0.06	Nickel	Ni	0.12
	Manganese	Mn	0.06	Manganese	Mn	0.12
	Magnesium	Mg	0.09	Magnesium	Mg	0.18
	Aluminium	Al	0.03	Aluminium	Al	0.06
	Copper	Cu	0.13	Copper	Cu	0.26
	Titanium	Ti	0.01	Titanium	Ti	0.02
Ion Chromatography	Sulphate	SO_4	1,966			
	Nitrate	NO_3	1,886	Nitrate	NO_3	3,772

The change in the element concentration as a function of time was also investigated. As shown in Figure 37, the gradual increment in the concentration of Na, Fe, Ni and Si indicates the gradual transfer of ions from the diluate to the concentrate.

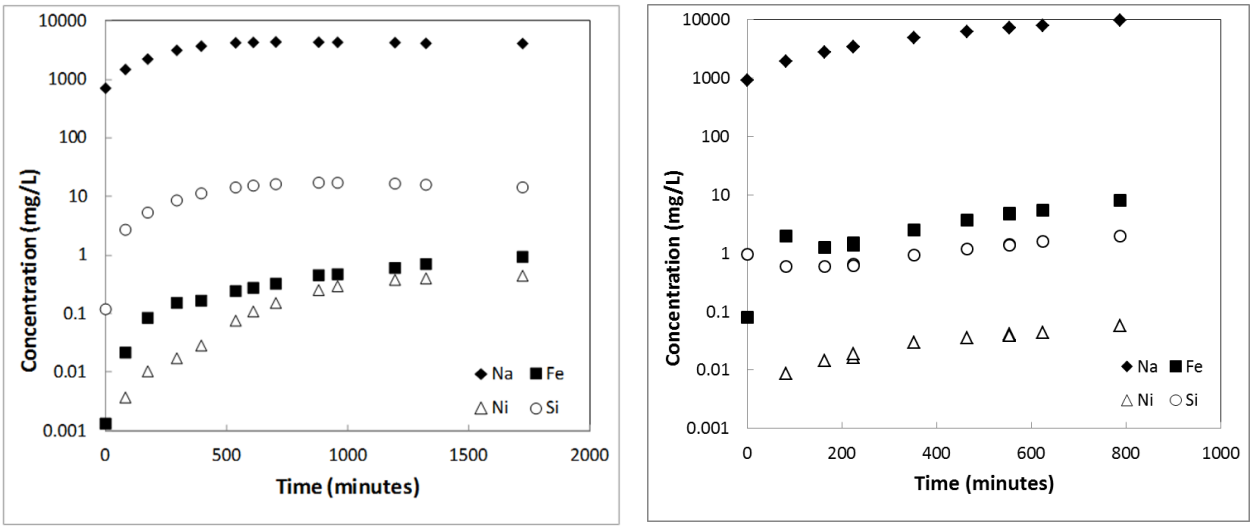

Figure 37 – Elemental analysis (Na, Fe, Ni and Si) of the concentrate in the (a) MF/ED MEA50+ and (b) MF/ED MEA 1800+

The amount of sulfate and nitrate transfer was also quantified using ion chromatography. Once again, the measurement was limited to the concentrate samples due to the limitation in the analysis method in the presence of high concentrations of MEA. As shown in Figure 38, there is also a gradual increase in sulfate and nitrate concentration as a function of time. The final concentrations are given in Table 9 and Table 10. The sulphate content measured by this approach (509 and 1966 ppm) is reasonably consistent with that calculated from the ICP sulfur analysis (612 and 1476 ppm) indicating that the main sulfur compound is indeed sulfate (SO_4^{2-} and not sulfite (SO_3^-).

It is readily apparent from this analysis that sulfates and nitrates represent the chief form of heat stable salts within the waste amine solvent, justifying our earlier focus on these anions in pure solutions. As discussed above, these are the salts after precipitation. Further analysis is required to determine the concentration of these salts before precipitation, but they are significantly higher.

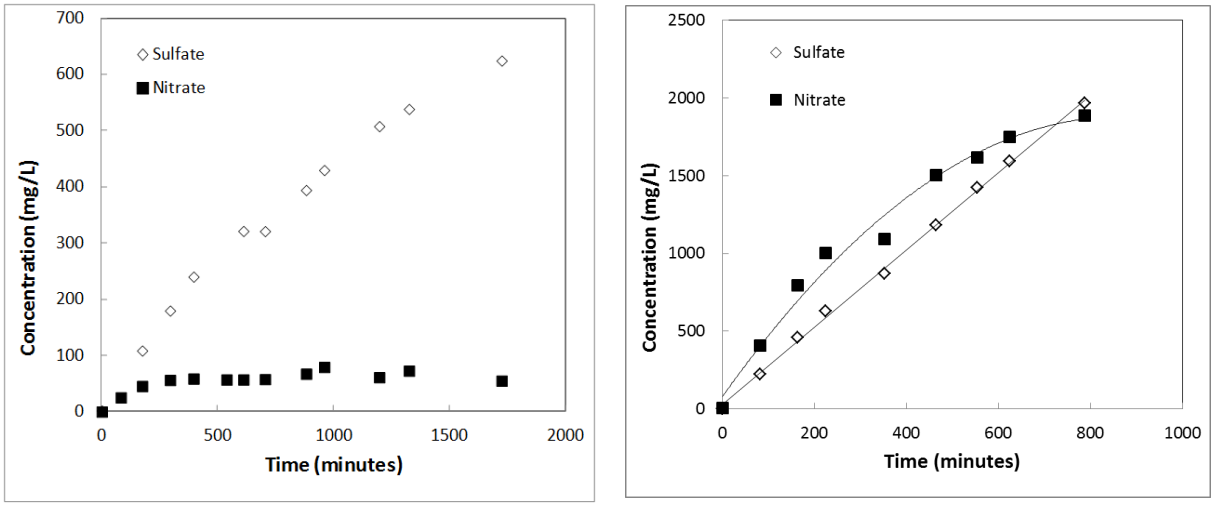

Figure 38 – Sulfate and nitrate concentration in the concentrate solution (a) MF/ED MEA50+ experiment) (b) MF/ED MEA 1800+

Additionally, MEA permeation across the ion-exchange membranes was confirmed by titration. As shown in Figure 39, permeation is evident from both the fall in the diluate concentration and the increase in the concentrate. The permeation rate estimated from the concentrate data is 0.16 g/m^2.s for the MEA50+ and 0.14 g/m^2.s for the MEA1800+; consistent with the estimate of 0.17 g/m^2.s estimated with the model solutions (Table 7). The protonated amine/carbamate anions moves across the membrane by preference to the free amine, so that the diluate becomes proportionately richer in free amine with time, while the concentrate contains a greater proportion of charged amines.

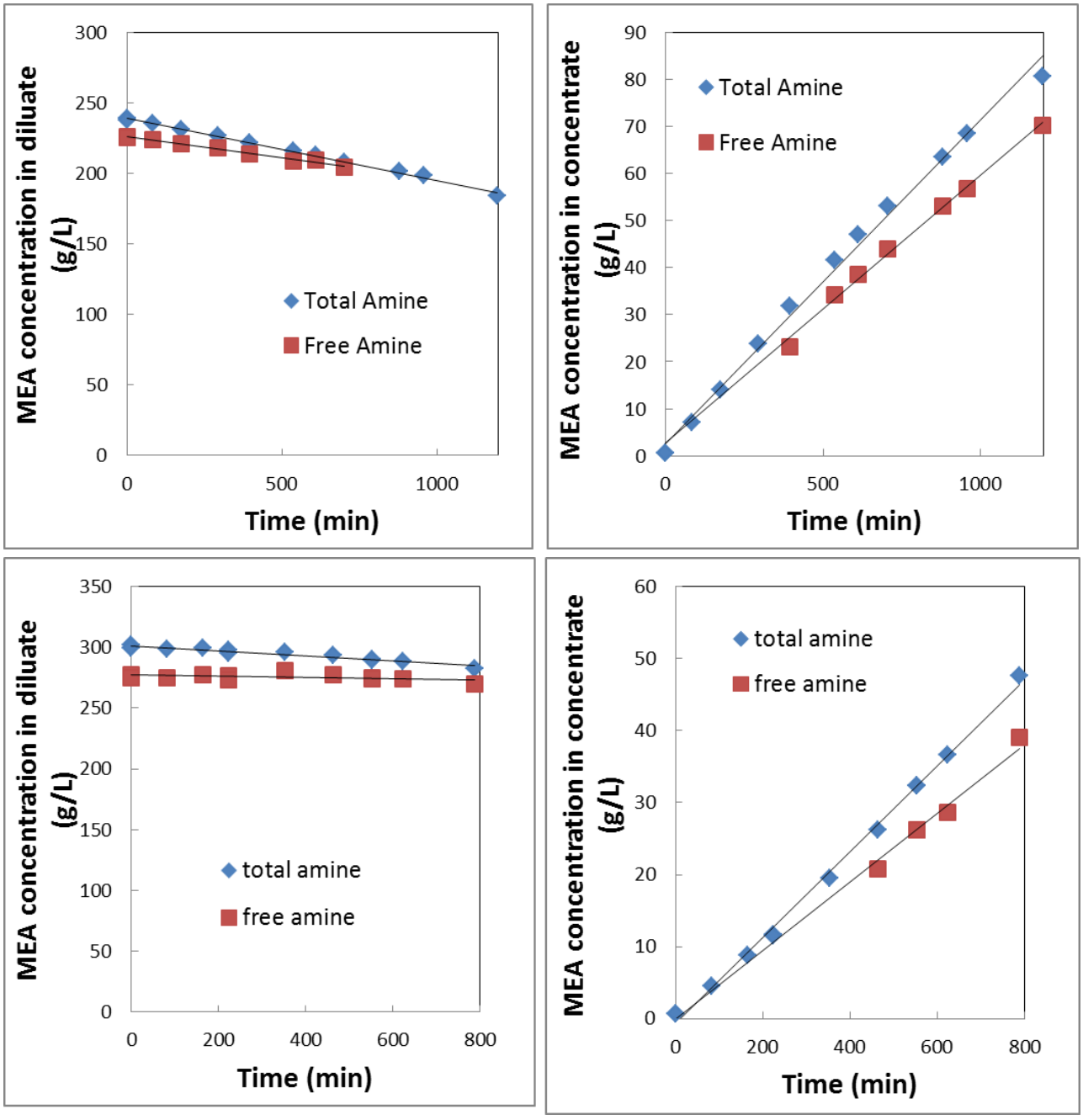

Figure 39 – MEA concentration in the diluate and concentrate solution (a) MEA50+ (b) MEA 1800+

The presence of MEA and other organic species was also confirmed qualitatively for the MEA 1800+ sample using NMR spectroscopy. The results are presented in Figure 40 and Figure 41. There is clear evidence of a range of organic contaminants, including MEA itself crossing the membranes into the concentrate.

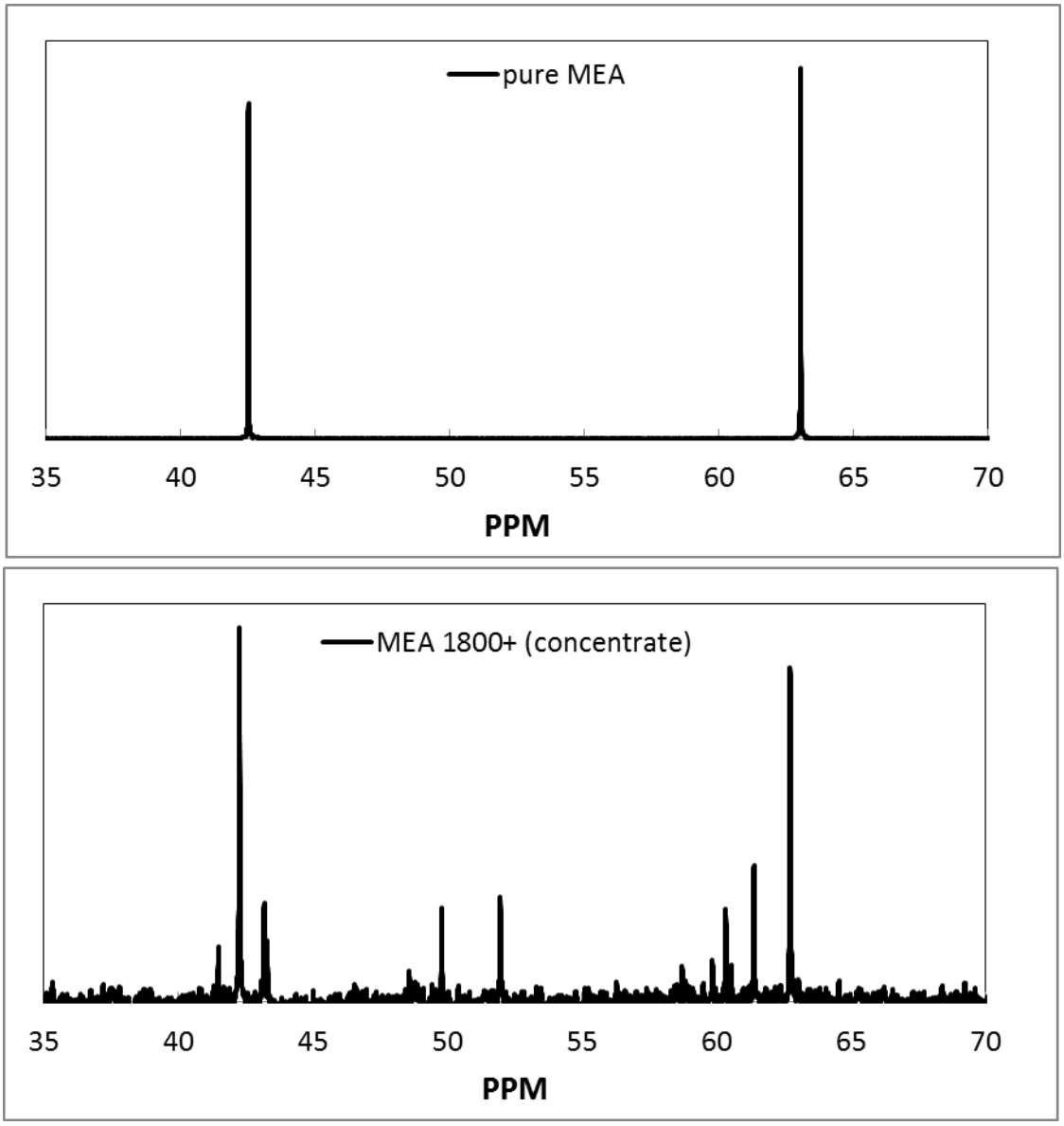

Figure 40 – ^{13}C NMR of a pure MEA solution and the MEA 1800+ Concentrate.

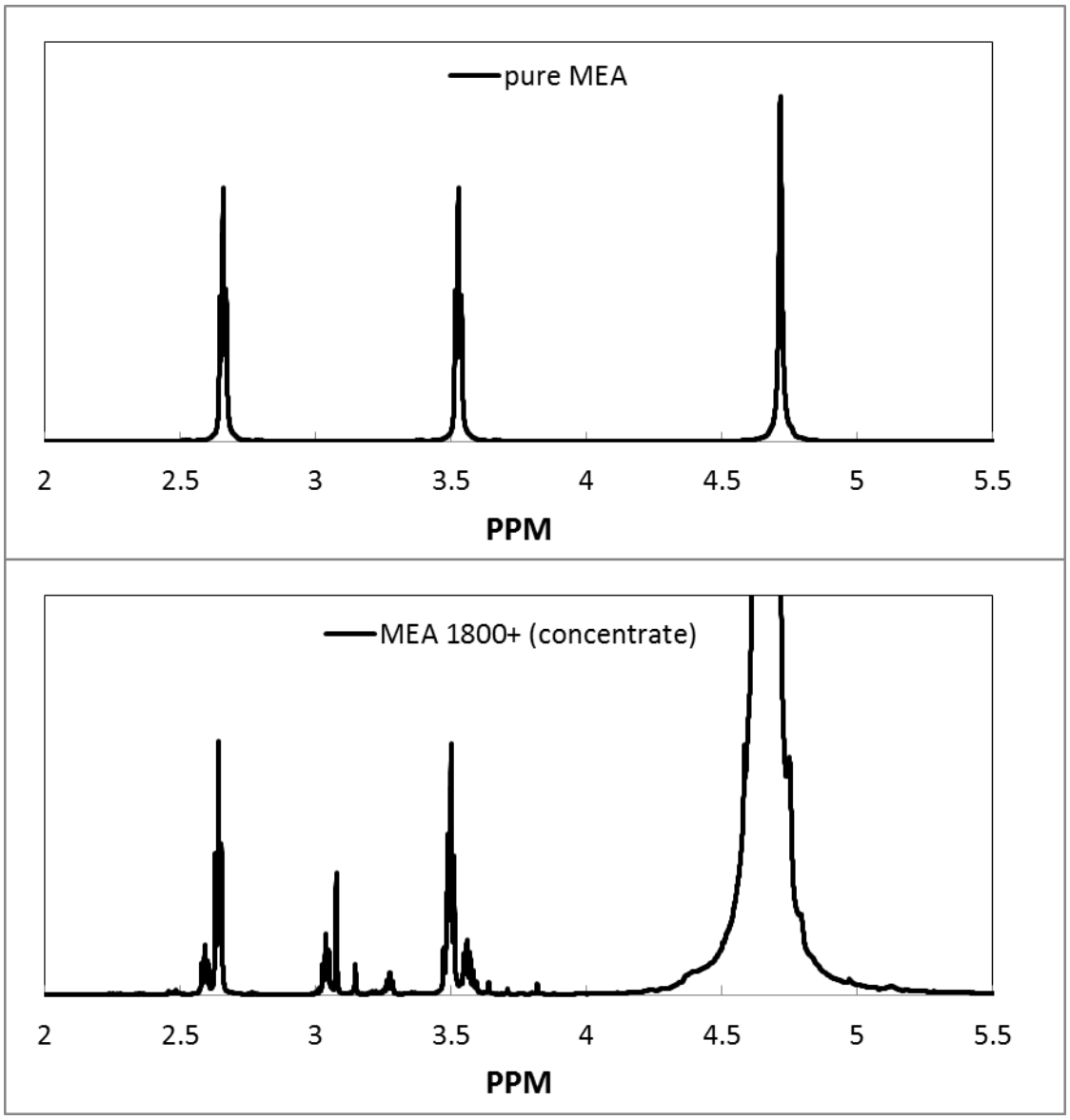

Figure 41 – ^{1}H NMR of a pure MEA solution and the MEA 1800+ Concentrate.

An additional run was conducted using the MEA 1800+ solution, in which the current density was changed at intervals (Figure 42). This experiment gave similar results to the earlier run, but the overall salt removal was higher due to the longer run time and higher current density at the end of the run (71 % based on diluate conductivity). There was no evidence that further ion depletion would not be possible with time.

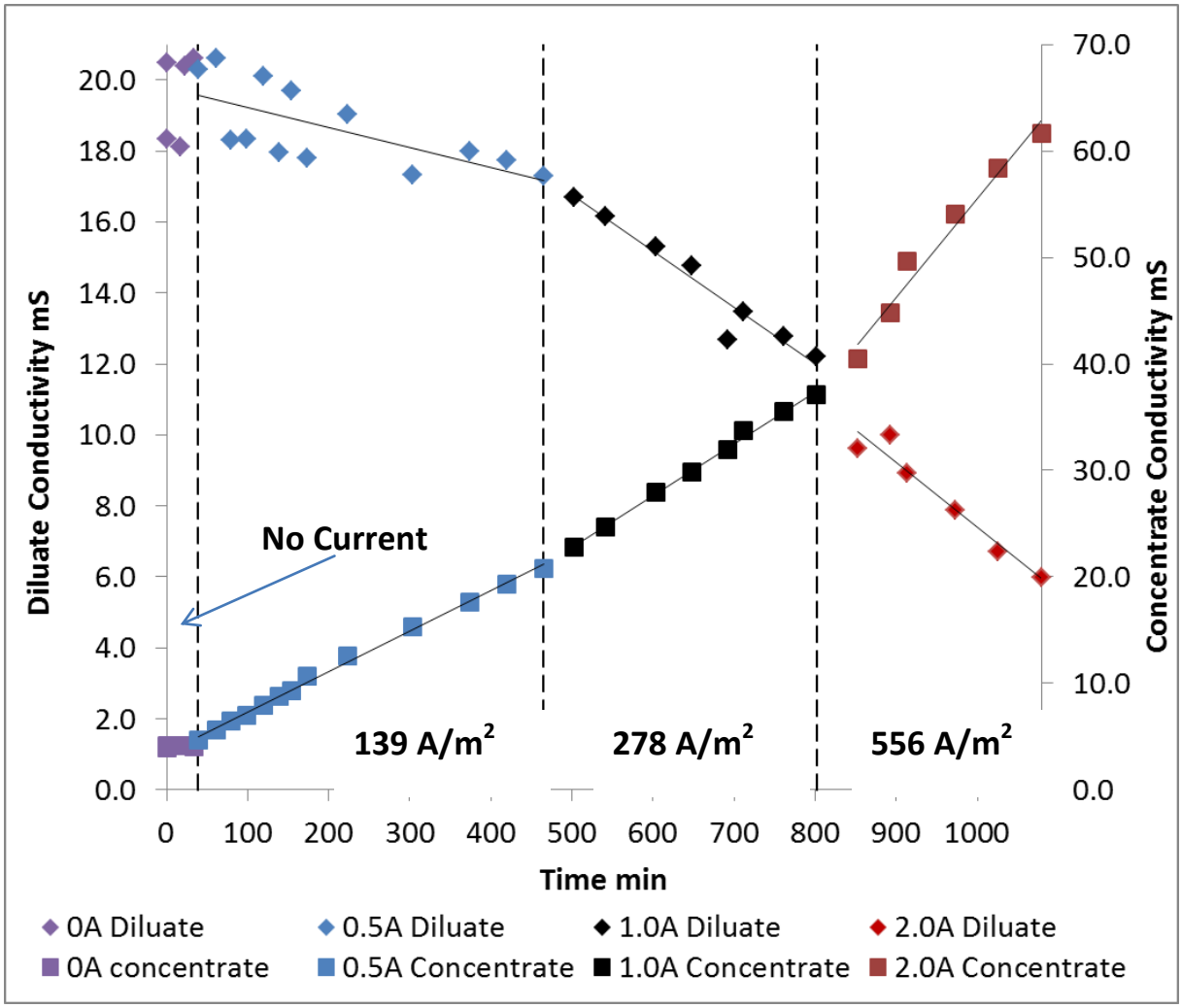

Figure 42 – The change in the diluate and concentrate solution conductivity over time (diluate = MEA1800+ after thermal boiling, neutralisation and microfiltration). The current density was varied from day to day.

Membrane stability for industrial solvent

The ATR-FTIR measurements (Figure 43 - Figure 45) show that MPF-34 and Neosepta CEM membranes are stable upon exposure to aged MEA solvent up to a period of 4.5 months. However, a slight change in the membrane composition of the Neosepta AEM is observed. The occurrence of the peaks at 1066 and 1351 cm^{-1} is probably related to the residue of MEA solution within the membrane and on the membrane surface. It was reported that the saturated primary alcohol C-O stretch absorption range is 1085-1050 cm^{-1}, and the interaction between O-H

bending and C-O stretching is at 1390-1330 cm^{-1} and 1260-1180 cm^{-1} [54]. The increase in peak height in the range 3000-3500 cm^{-1} is indicative of water sorption (see Figure 9).

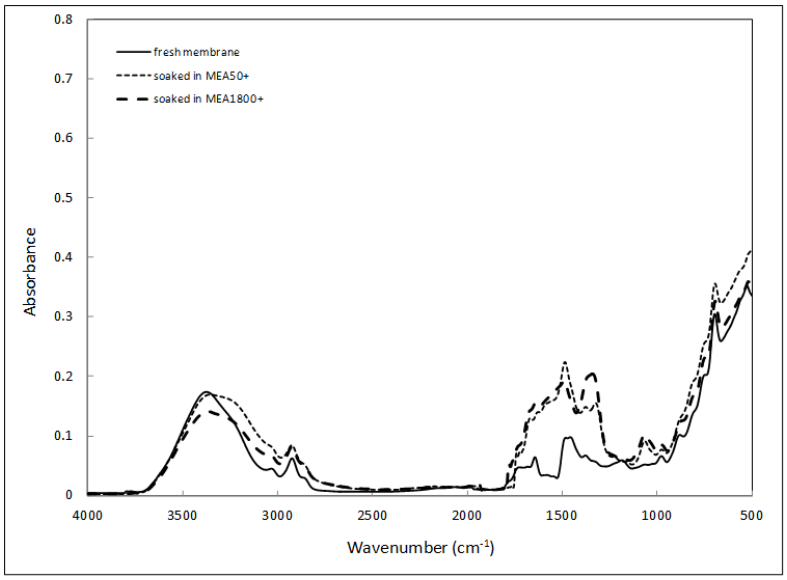

Figure 43 – The ATR-FTIR spectra for Neosepta anion exchange membranes soaked in aged industrial solvents

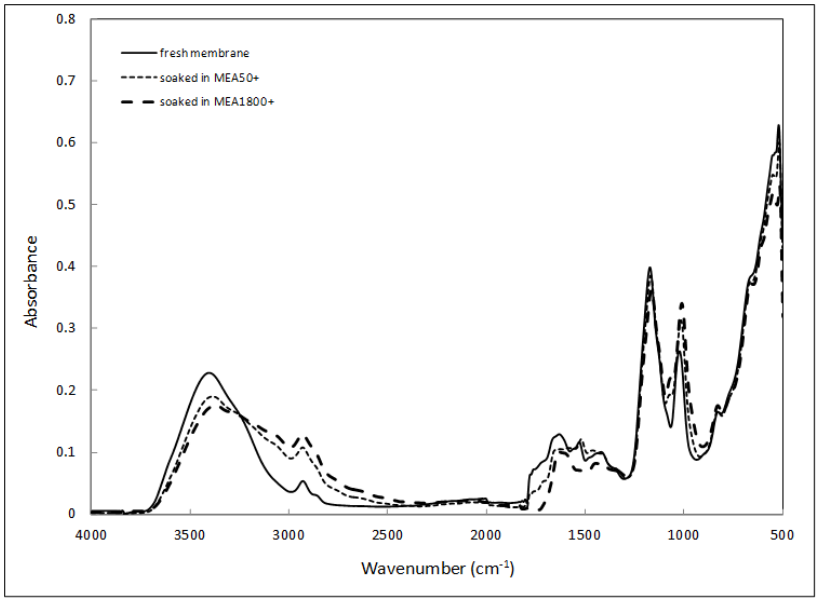

Figure 44 – The ATR-FTIR spectra for Neosepta cation exchange membranes soaked in aged industrial solvents

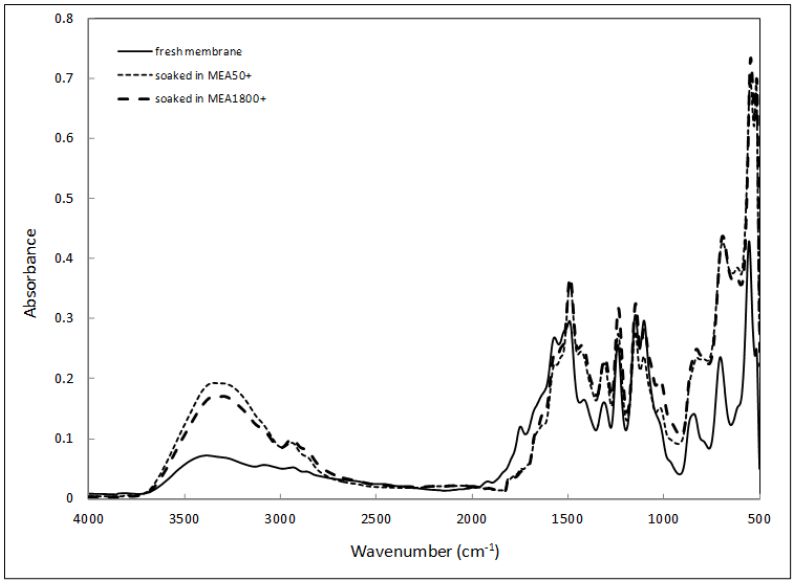

Figure 45 – The ATR-FTIR spectra for Koch MPF-34 membranes soaked in aged industrial solvents

Conclusions

This project has clearly shown the potential of electrodialysis as a mechanism to purify MEA solvents during carbon capture applications. Up to 92 % of the heat stable salts has been removed from an industrial aged MEA solvent using this approach. We found the Astom Neosepta AHA and CMB membranes the most effective for this application, although the Fumatech Fumasep FAB/FKB pair also showed potential. The choice of operating conditions, and specifically the current density selected for such an operation will be a balance between operating and capital costs. Low current densities lead to high current efficiencies, which reduce the overall energy demand. However, at these lower current densities, more membrane area will be required adding to capital costs.

Nanofiltration was also investigated in this project. This approach proved highly effective on model pure solutions, as a mechanism to concentrate the heat stable salts. In this mode, a nanofiltration pretreatment step could facilitate more effective electrodialysis, by increasing the total salt concentration here, while minimizing corrosion by minimizing salt concentration in the main solvent plant. However, the approach proved less effective on industrial aged solvent, probably as a result of the non-zero CO_2 loading. If this approach were to be successful, it is likely to require additional stripping as a pre-treatment to reduce this loading.

The principal heat stable salts detected in the aged solvent from the Loy Yang power station were sulfate and nitrate salts, most likely formed from reactions of the amine solvents with SO_x and NO_x. Metal salts, such as can occur as a corrosion byproduct, were relatively minimal.

Recommendations for Further Work

The work presented here was conducted in a ‘batch mode’ on aged solvent that was already substantially contaminated. In a full scale capture operation, it is likely to be more practical and economically effective to run a continuous operation on a slipstream of cool, lean solvent as suggested in Figure 1. The next step towards development of a commercial process should thus be to run a pilot scale operation on an operating carbon capture plant using the Neosepta membranes. This would allow flowrates, CO_2 loadings and current densities to be optimized to provide the most practical, cost effective and energy efficient operation.

Further, the work considered only MEA as solvent. While this is the current benchmark solvent, a range of alternative amines and amino acid solvents are under consideration internationally. The work completed here should be extended to such novel solvents.

Finally, time and analytical capability did not allow a thorough investigation of the nature of the precipitates formed during the neutralization step, or the chemical composition of the diluate solution. This analysis should be completed.

References

[1] C. Stewart, M.-A. Hessami, A study of methods of carbon dioxide capture and sequestration—the sustainability of a photosynthetic bioreactor approach, Energy Conversion and Management, 46 (2005) 403-420.

[2] H. Yang, Z. Xu, M. Fan, R. Gupta, R.B. Slimane, A.E. Bland, I. Wright, Progress in carbon dioxide separation and capture: A review, Journal of Environmental Sciences, 20 (2008) 14-27.

[3] H. Lepaumier, D. Picq, P.-L. Carrette, New Amines for CO_2 Capture. I. Mechanisms of Amine Degradation in the Presence of CO_2, Industrial & Engineering Chemistry Research, 48 (2009) 9061-9067.

[4] J.M. Plaza, D. Van Wagener, G.T. Rochelle, Modeling CO_2 capture with aqueous monoethanolamine, International Journal of Greenhouse Gas Control, 4 (2010) 161-166.

[5] R. Strube, G. Pellegrini, G. Manfrida, The environmental impact of post-combustion CO_2 capture with MEA, with aqueous ammonia, and with an aqueous ammonia-ethanol mixture for a coal-fired power plant, Energy, 36 (2011) 3763-3770.

[6] P.C. Rooney, T.R. Bacon, M.S. DuPart, Effect of heat stable salts on MDEA solution corrosivity Parts 1&2, in: Hydrocarbon Processing, Gulf Publishing Co., Houston, Texas, 1996, pp. 95-103.

[7] W. Tanthapanichakoon, J. Gale, Heat Stable Salts and Corrosivity in Amine Treating Units, in: Greenhouse Gas Control Technologies - 6th International Conference, 2003, pp. 1591.

[8] N. Verma, A. Verma, Amine system problems arising from heat stable salts and solutions to improve system performance, Fuel Processing Technology, 90 (2009) 483-489.

[9] L. Dumée, C. Scholes, G. Stevens, S. Kentish, Purification of aqueous amine solvents used in post combustion CO_2 capture: A review, International Journal of Greenhouse Gas Control, 10 (2012) 443-455.

[10] P.C. Rooney, T.R. Bacon, M.S. DuPart, Effect of heat stable salts on MDEA solution corrosivity, Hydrocarbon Processing, 76 (1997) 65-70.

[11] S. Chi, G.T. Rochelle, Oxidative Degradation of Monoethanolamine, Industrial & Engineering Chemistry Research, 41 (2002) 4178-4186.

[12] J. Davis, A. Sexton, Amine degradation, in: 11th Meeting of the International CO2 Capture Test Network, Vienna, Austria, 2008.

[13] R. Steeneveldt, B. Berger, T.A. Torp, CO_2 Capture and Storage: Closing the Knowing–Doing Gap, Chemical Engineering Research and Design, 84 (2006) 739-763.

[14] J.C.M. Pires, F.G. Martins, M.C.M. Alvim-Ferraz, M. Simoes, Recent developments on carbon capture and storage: An overview, Neuere Entwicklungen bei Kohlendioxidentfernung und Kohlendioxidlagerung: Eine Übersicht, (2012) 1446.

[15] P.C. Rooney, Amine heat stable salt neutralization having reduced solids, United States Patent No. 5912387 The Dow Chemical Company, 1999.

[16] B. Thitakamol, A. Veawab, A. Aroonwilas, Environmental impacts of absorption-based CO_2 capture unit for post-combustion treatment of flue gas from coal-fired power plant, International Journal of Greenhouse Gas Control, 1 (2007) 318-342.

[17] A.L. Kohl, R. Nielsen, Gas purification, Gulf Publishing, Houston, Texas, 1997.

[18] D. Burns, R.A. Gregory, The UCARSEP® Process for On-Line Removal of Non-Regenerable Salts from Amine Units, Proceeding of Laurence Reid Gas Conditioning Conference, Norman Oklahoma, 1995.

[19] S.A. Bedell, S.S.K. Tsai, Process for the recovery of alkanolamines from their heat-stable salts formed in alkanolamine sorbent solutions, US Patent No. 4814051, The Dow Chemical Company, 1989.

[20] R.A. Gregory Jr., M.F. Cohen, Aqueous alkanolamines using an electrodialysis cell with an ion exchange membrane, in: United States Patent No. 5,910,611, Union Carbide Chemicals & Plastics Technology Corporation (Danbury, CT) United States 1999.

[21] B. Van der Bruggen, M. Mänttäri, M. Nyström, Drawbacks of applying nanofiltration and how to avoid them: A review, Separation and Purification Technology, 63 (2008) 251-263.

[22] M. Mänttäri, K. Viitikko, M. Nyström, Nanofiltration of biologically treated effluents from the pulp and paper industry, Journal of Membrane Science, 272 (2006) 152-160.

[23] J.M. Gozálvez-Zafrilla, D. Sanz-Escribano, J. Lora-García, M.C. León Hidalgo, Nanofiltration of secondary effluent for wastewater reuse in the textile industry, Desalination, 222 (2008) 272-279.

[24] W.-J. Lau, A.F. Ismail, Polymeric nanofiltration membranes for textile dye wastewater treatment: Preparation, performance evaluation, transport modelling, and fouling control — a review, Desalination, 245 (2009) 321-348.

[25] S.C. Low, C. Liping, L.S. Hee, Water softening using a generic low cost nano-filtration membrane, Desalination, 221 (2008) 168-173.

[26] K. Listiarini, J.T. Tor, D.D. Sun, J.O. Leckie, Hybrid coagulation–nanofiltration membrane for removal of bromate and humic acid in water, Journal of Membrane Science, 365 (2010) 154-159.

[27] T.J.K. Visser, S.J. Modise, H.M. Krieg, K. Keizer, The removal of acid sulphate pollution by nanofiltration, Desalination, 140 (2001) 79-86.

[28] R. Chalatip, R. Chawalit, R. Nopawan, Removal of haloacetic acids by nanofiltration, Journal of Environmental Sciences, 21 (2009) 96-100.

[29] A.V. Volkov, G.A. Korneeva, F.T. Gennadii, Organic solvent nanofiltration: prospects and application, Russian Chemical Reviews, 77 (2008) 983.

[30] S. Binyam, H. Mukhtar, L. Leong, Flux and rejection of monoethanolamine (MEA) in wastewater using membrane technology Thirteenth International Water Technology Conference, Hurghada, Egypt, 2009.

[31] A.L. Cummings, F.C. Veatch, A.E. Keller, S.M. Mecum, R.M. Kammiller, An analytical method for determining bound and free alkanolamines in heat stable salt contaminated solutions, in: AIChE 1990 Summer National Meeting Symposium on Gas Processing, Ponca City, OK, 1990.

[32] T.G. Amundsen, L.E. Øi, D.A. Eimer, Density and viscosity of monoethanolamine+ water+ carbon dioxide from (25 to 80) C, Journal of Chemical & Engineering Data, 54 (2009) 3096-3100.

[33] G. Artuğ, I. Roosmasari, K. Richau, J. Hapke, A comprehensive characterization of commercial nanofiltration membranes, Separation Science and Technology, 42 (2007) 2947-2986.

[34] T. Hoang, G. Stevens, S. Kentish, The effect of feed pH on the performance of a reverse osmosis membrane, Desalination, 261 (2010) 99-103.

[35] G. Artug, J. Hapke, Characterization of nanofiltration membranes by their morphology, charge and filtration performance parameters, Desalination, 200 (2006) 178-180.

[36] S. Bandini, J. Drei, D. Vezzani, The role of pH and concentration on the ion rejection in polyamide nanofiltration membranes, Journal of Membrane Science, 264 (2005) 65-74.

[37] S. Bandini, D. Vezzani, Nanofiltration modeling: the role of dielectric exclusion in membrane characterization, Chemical Engineering Science, 58 (2003) 3303-3326.

[38] M. Dalwani, N.E. Benes, G. Bargeman, D. Stamatialis, M. Wessling, Effect of pH on the performance of polyamide/polyacrylanitrile based thin film composite membranes, Journal of Membrane Science, 372 (2011) 228-238.

[39] J.-H. Choi, K. Fukushi, K. Yamamoto, A study on the removal of organic acids from wastewaters using nanofiltration membranes, Separation and Purification Technology, 59 (2008) 17-25.

[40] B. Van der Bruggen, A. Koninckx, C. Vandecasteele, Separation of monovalent and divalent ions from aqueous solution by electrodialysis and nanofiltration, Water research, 38 (2004) 1347-1353.

[41] M. Mänttäri, A. Pihlajamäki, M. Nyström, Effect of pH on hydrophilicity and charge and their effect on the filtration efficiency of NF membranes at different pH, Journal of Membrane Science, 280 (2006) 311-320.

[42] R.H. Weiland, J.C. Dingman, D.B. Cronin, G.J. Browning, Density and viscosity of some partially carbonated aqueous alkanolamine solutions and their blends, Journal of Chemical & Engineering Data, 43 (1998) 378-382.

[43] G. Kraaijeveld, V. Sumberova, S. Kuindersma, H. Wesselingh, Modelling electrodialysis using the Maxwell-Stefan description, The Chemical Engineering Journal and The Biochemical Engineering Journal, 57 (1995) 163-176.

[44] M. Demircioglu, N. Kabay, I. Kurucaovali, E. Ersoz, Demineralization by electrodialysis (ED)—separation performance and cost comparison for monovalent salts, Desalination, 153 (2003) 329-333.

[45] J. Stodollick, R. Femmer, M. Gloede, T. Melin, M. Wessling, Electrodialysis of itaconic acid: A short-cut model quantifying the electrical resistance in the overlimiting current density region, Journal of Membrane Science, 453 (2014) 275-281.

[46] P. Długołęcki, B. Anet, S.J. Metz, K. Nijmeijer, M. Wessling, Transport limitations in ion exchange membranes at low salt concentrations, Journal of Membrane Science, 346 (2010) 163-171.

[47] I. Rubinstein, B. Zaltzman, Electro-osmotically induced convection at a permselective membrane, Physical Review E, 62 (2000) 2238-2251.

[48] S.M. Rubinstein, G. Manukyan, A. Staicu, I. Rubinstein, B. Zaltzman, R.G.H. Lammertink, F. Mugele, M. Wessling, Direct Observation of a Nonequilibrium Electro-Osmotic Instability, Physical Review Letters, 101 (2008) 236101.

[49] R. Simons, Water splitting in ion exchange membranes, Electrochimica Acta, 30 (1985) 275-282.

[50] Y. Tanaka, Water dissociation reaction generated in an ion exchange membrane, Journal of Membrane Science, 350 (2010) 347-360.

[51] S. Thampy, P. Narayanan, W. Harkare, K. Govindan, Seawater desalination by electrodialysis. Part II: a novel approach to combat scaling in seawater desalination by electrodialysis, Desalination, 69 (1988) 261-273.

[52] M. Kameche, F. Xu, C. Innocent, G. Pourcelly, Z. Derriche, Characterisation of Nafion® 117 membrane modified chemically with a conducting polymer: An application to the demineralisation of sodium iodide organic solutions, Separation and Purification Technology, 52 (2007) 497-503.

[53] S.E. Kentish, E. Kloester, G.W. Stevens, C.A. Scholes, L. Dumée, Electrodialysis in aqueous-organic mixtures, Separation and Purification Reviews, submitted (2013).

[54] R. Silverstein, F. Webster, Spectrometric identification of organic compounds, John Wiley & Sons, 2006.

Summary of outcomes

The Gantt chart for the project is presented in Table 11. The project was extended for three months due to a delay in obtaining the aged industrial solvent. Overall, all the milestones were completed successfully.

Table 11 - Gantt chart of the project (Y - completed, N – not completed)

Key Milestones	Tasks	Q1 2011	Q2 2011	Q3 2011	Q4 2011	Q1 2012	Q2 2012	Q3 2012	Q4 2012	Q1 2013	Q2 2013	Q3 2013	Q4 2013	Q1 2014	COMPLETED?
1. Signing of Contracts															Y
2. Human Resources Employed	Early advertisement and recruitment														Y
3. Test facilities in place	Nanofiltration / electrodialysis review and development of experimental rig														Y
4. Test program and data collection (Stage Gate 1)	Commence experiments on membrane filtration using model contaminant solutions														Y
	Dissemination of early results through presentations														Y
5. Advanced Membrane Testing (Stage Gate 2)	Complete experiments on membrane filtration using model contaminant solutions														Y
6. Data analysis complete	Conduct membrane experiments using waste amine solvents from pilot or full scale trials														Y
7.Dissemination activities	Final Journal and conference publications														Y
8. Final Report	Final Report prepared and submitted incorporating all results obtained.														Y

CONTACT US

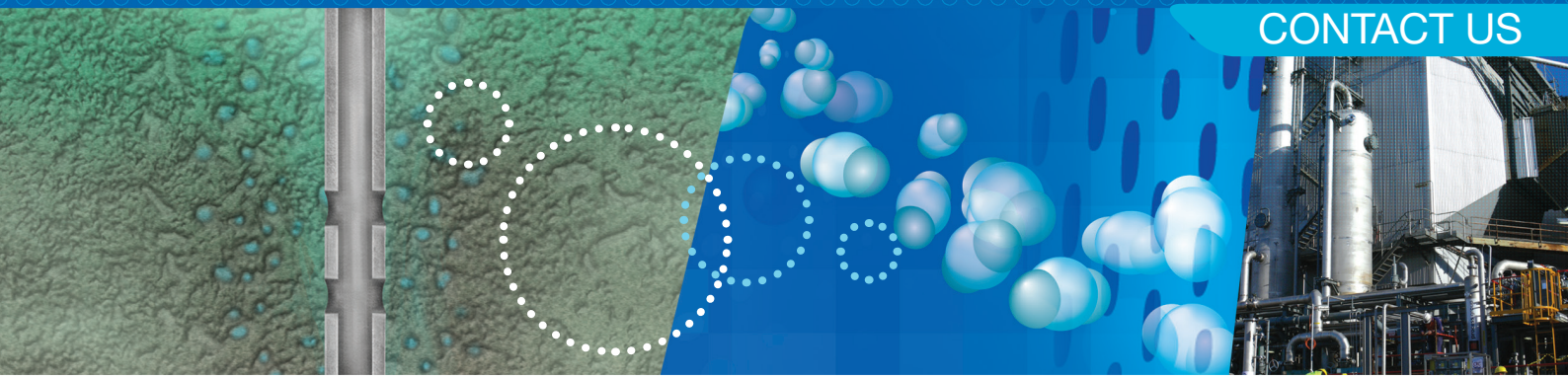

Canberra

Dr Richard Aldous
Chief Executive

GPO Box 463, Canberra, ACT 2601
Ph: + 61 2 6120 1600
Fax: + 61 2 6273 7181
Email: raldous@co2crc.com.au

Ms Carole Peacock
Business Manager

GPO Box 463, Canberra, ACT 2601
Ph: + 61 2 6120 1605
Fax: + 61 2 6273 7181
Email: cpeacock@co2crc.com.au

Melbourne

Dr Matthias Raab
Program Manager for CO_2 Storage

School of Earth Science
The University of Melbourne
VIC 3010
Ph: +61 3 8344 4309
Fax: +61 3 8344 7761
Email: mraab@co2crc.com.au

Mr Rajindar Singh
Otway Operations Manager

School of Earth Science
The University of Melbourne
VIC 3010
Ph: + 61 3 8344 9007
Fax: + 61 3 8344 7761
Email: rssingh@co2crc.com.au

Sydney

Prof Dianne Wiley
Program Manager for CO_2 Capture

The University of New South Wales
UNSW Sydney, 2052
Ph: + 61 2 9385 4755
Email: dwiley@co2crc.com.au

Adelaide

Prof John Kaldi
Chief Scientist

Australian School of Petroleum
The University of Adelaide, SA 5005
Ph: + 61 8 8303 4291
Fax: + 61 8 8303 4345
Email: jkaldi@co2crc.com.au

Perth

Mr David Hilditch
Commercial Manager (CO2TECH)

PO Box 1130, Bentley
Western Australia 6102
Ph: + 61 8 6436 8655
Fax: + 61 8 6436 8555
Email: dhilditch@co2crc.com.au

researching carbon capture and storage